CT 74-13

NASA CR-

141676

# SPACE SHUTTLE MANEUVERING ENGINE

# REUSABLE THRUST CHAMBER PROGRAM

NAS9-12802

## Task XI
## Stability Analyses and
## Acoustic Model Testing
## Data Dump

December 1974

Prepared by

C. L. Oberg
Combustion Technology
Advanced Programs

APPROVED BY:

R. P. Pauckert
SS/OME Principal Engineer
Advanced Projects

R. D. Paster
Acting Program Manager
SS/OME Program

ROCKETDYNE DIVISION, ROCKWELL INTERNATIONAL
6633 Canoga Avenue
Canoga Park, California 91304

# NOMENCLATURE



## Arabic Symbols

$C_c$ = contraction coefficient for orifice

$c$ = sound velocity

$g_c$ = mass/force units conversion constant (32.2 lbm ft/lbf $sec^2$)

$J_m(x)$ = Bessel function of first kind and order m

$j$ = $(-1)^{\frac{1}{2}}$

$k$ = $\omega/c$

$k_{mn}$ = $(k^2 - \alpha_{mn}^2/r_w^2)^{\frac{1}{2}}$

$L$ = chamber length

$\ell$ = orifice length

$m$ = circumferential mode index

$\tilde{p}$ = oscillatory pressure

$r$ = radial position coordinate

$r_w$ = radius of wall

$S$ = cross-section area

$\tilde{u}$ = oscillatory velocity

$\bar{u}_o$ = steady flow velocity in orifice

$Z$ = acoustic impedance

$z$ = axial position coordinate

## Greek Symbols

$\alpha_{mn}$ = root of Bessel function, $dJ_m(\alpha_{mn})/d\alpha_{mn} = 0$

$\delta$ = length end correction

$\theta$ = angular coordinate; also, specific acoustic resistance

$\rho$ = time averaged gas density

$\sigma$ = fractional open area

$\chi$ = specific acoustic reactance

$\omega$ = angular frequency

Subscripts

i = denotes region i

u = denotes upstream side of orifice

D = denotes downstream side of orifice

Superscripts

i = denotes region i

- = denotes time-averaged value

# INTRODUCTION AND SUMMARY

The purpose of the study described herein was to investigate the combustion stability characteristics of engines applicable to the Space Shuttle Orbit Maneuvering System and the adequacy of acoustic cavities as a means of assuring stability in these engines. The study comprised full-scale stability rating tests, bench-scale acoustic model tests and analysis. Two series of stability rating tests were made.

The objective of the first series of tests, made with an 8.2-inch-diameter chamber having a contraction ratio of 2.0, was to determine the acoustic cavity entrance configuration required to assure stability and, also, to assess the effects of a change in boundary layer coolant (BLC) injection on stability. The objective of the second series of stability rating tests, made with a 10-inch-diameter chamber having a contraction ratio of 3.0, was to determine the stability characteristics of a new injector designed for a chamber of this size.

Acoustic model tests were made to determine the resonance characteristics and effects of acoustic cavities.

Analytical studies were done to aid design of the cavity configurations to be tested and, also, to aid evaluation of the effectiveness of acoustic cavities from available test results.

## SUMMARY OF PRINCIPAL CONCLUSIONS

Test results show that the low contraction-ratio (8.2-inch diameter) chamber with the L/D #1 (also L/D #2) injector is adequately stabilized with a contoured entrance cavity without overlap (between the chamber wall and the inner wall of the cavity).

The high contraction ratio (10-inch diameter) chamber with the L/D #4 injector was stabilized with a similar cavity, and this hardware combination appears more stable than the low-contraction-ratio combination.

Acoustic model tests have been used to characterize the resonance characteristics of a relatively wide range of cavity configurations.

With many cavity configurations, a 2300 to 2900 Hz mode of oscillation dominates the stability characteristics of the 8-inch-diameter chamber. This mode has not been identified fully but is probably associated with the acoustics of the feed system with some chamber/cavity interaction. Additional effort is needed to develop effective methods of suppressing this mode.

## FULL-SCALE STABILITY RATING TESTS

### LOW CONTRACTION RATIO CHAMBER

A series of full-scale stability rating tests was made with an 8.2-inch diameter chamber which had a contraction ratio of 2.0 and an injector-to-throat distance of 16 inches. Results from these tests have been described previously (Ref. 1) but will be outlined here as well. These tests were made with the Rocketdyne like-doublet No. 1 (L/D #1) injector. This injector has 186 like-doublet elements (each comprising two oxidizer and two fuel orifices) arranged in 9 circular rows. The fuel and oxidizer orifice sizes range from 0.028 to 0.033 and 0.032 to 0.038 inches, respectively. BLC was injected along the periphery of the injector through 68 axially directed 0.020-inch diameter orifices. The nominal BLC flowrate was 2.7 percent of the total propellant flow.

The solid-wall chamber configuration is illustrated (with important exceptions) in Fig. 1. The exceptions are: An 8-inch-long cylindrical chamber section was actually used, rather than the 4-inch-long section shown. The BLC injector was replaced by a modified fuel manifold and acoustic cavity ring assembly. The acoustic cavities were located in the region shown but were formed from a replaceable two-part ring assembly which replaced the outer portion of the injector.

A photograph of the L/D #1 injector is shown in Fig. 2. This injector had been used previously for extensive non-stability-related testing, although a few stability rating tests had been made before the BLC injection orifices were drilled in the injector. These tests were stable with the acoustic cavity being used. Related stability rating tests had been made with a somewhat similar injector, L/D #2, which showed that an acoustic cavity was required to achieve stability (Ref. 2).

The chamber was instrumented with three high-frequency response pressure transducers, either Kistler model 614B/644 or PCB Piezotronics Model 123A helium and water-cooled transducers. These were located 2.82 inches downstream from the injector face at three different angular locations, $108^{o}$, $228^{o}$, and $276^{o}$ (referred to fuel inlet). The high-frequency data were

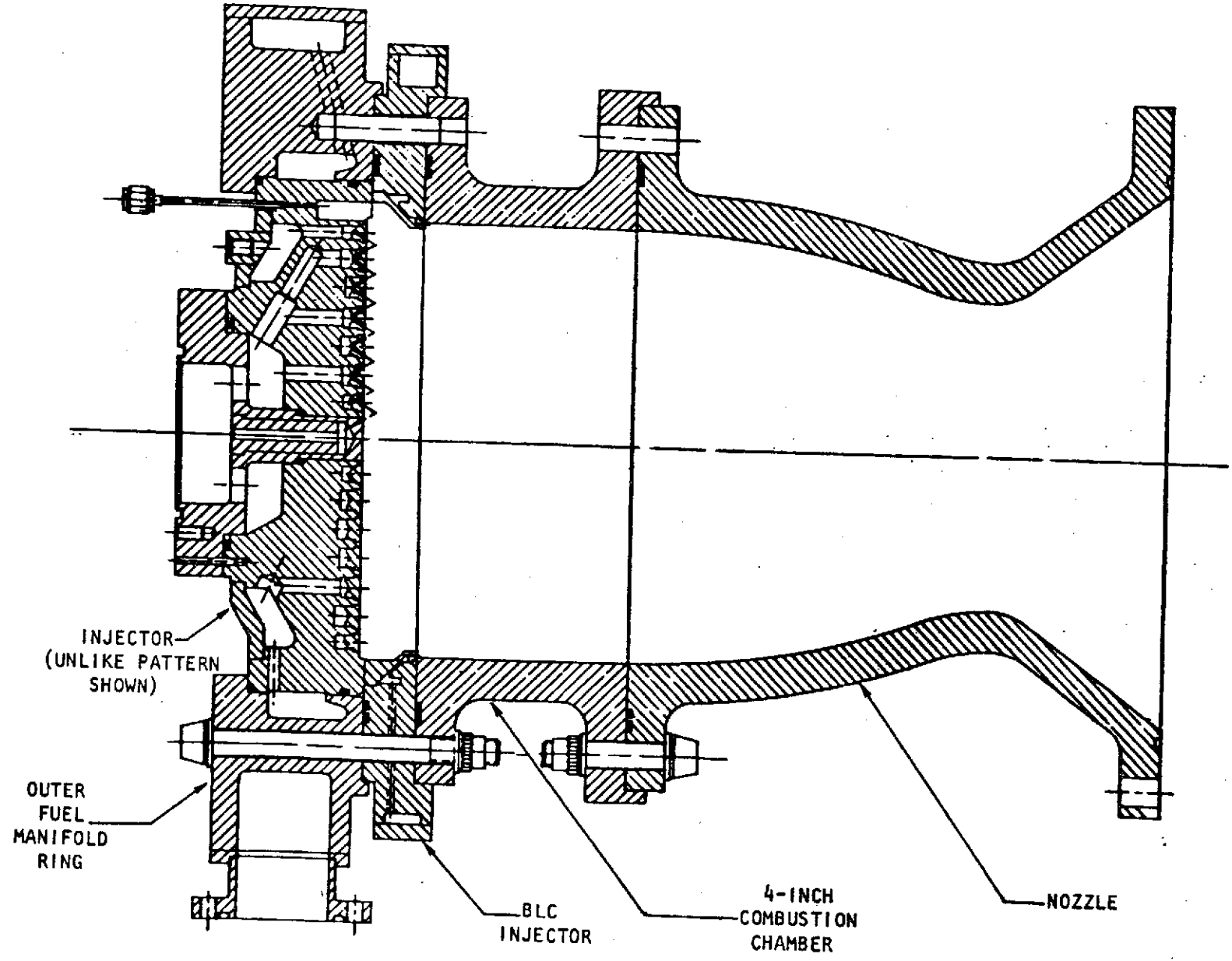


FIGURE 1. APPROXIMATE CONFIGURATION OF THRUST CHAMBER ASSEMBLY USED FOR TESTING

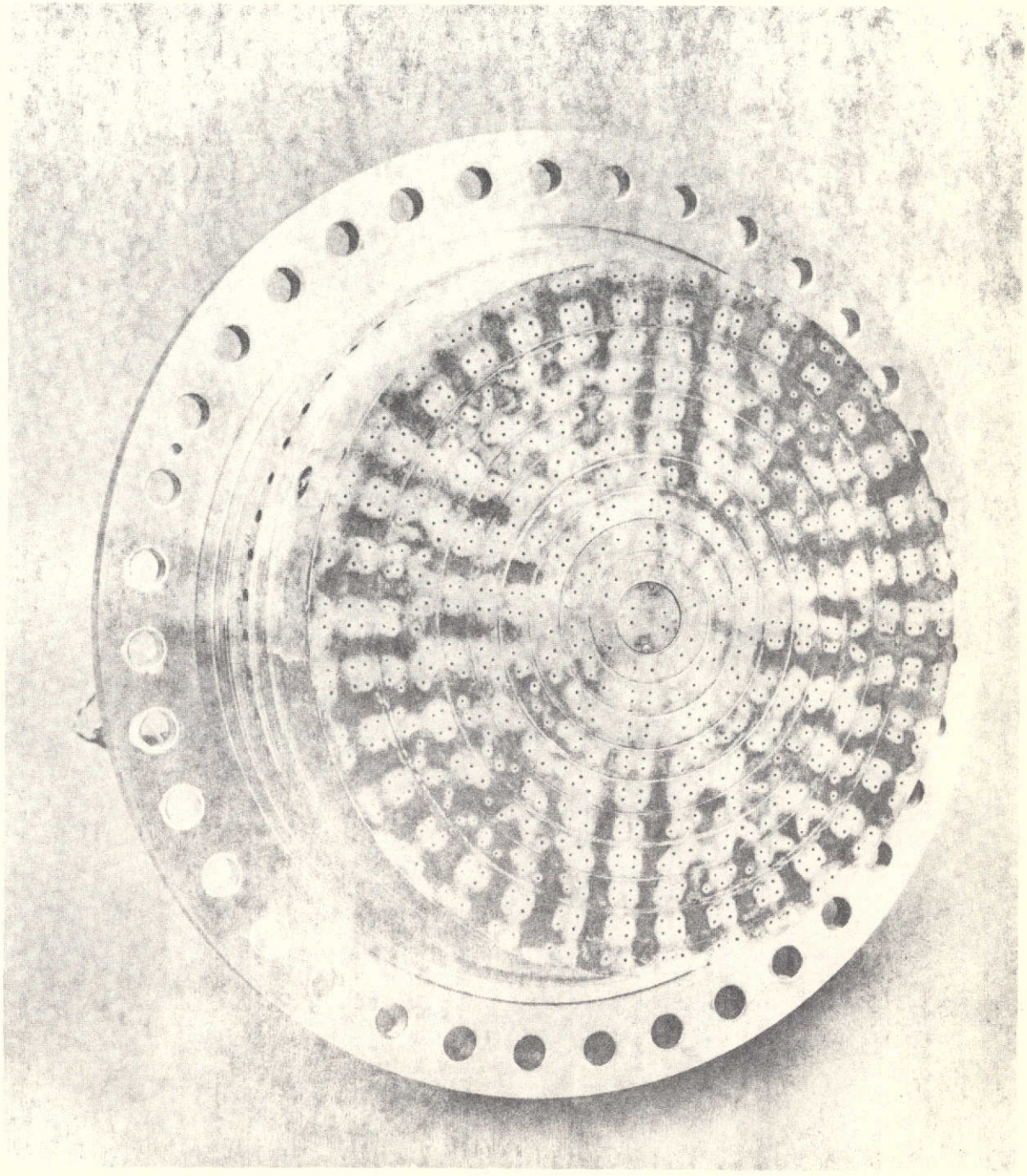



FIGURE 2. PHOTOGRAPH OF LIKE-DOUBLET NO. 1 INJECTOR

recorded on magnetic tape for subsequent analysis. The stability rating bombs were located at the same axial position and angular locations of $60^{0}$ and $324^{0}$. Two cork insulated 6½ grain (6½ grains RDX and 500 milligrams lead azide) bombs were used for each firing.

Gas temperatures were measured in the acoustic cavities with exposed-junction tungsten/rhenium (W-5% Rh/W-26% Rh) or chromel-alumel thermocouples depending on the location (temperature).

Stability results from the testing with the 8.2-inch-diameter chamber are summarized in Table 1. Each entry in this table corresponds to a single test but two bomb disturbances, generally.

The acoustic cavities used for all of these tests had a contoured (or fully contoured) entrance, illustrated below. If difficulty had been encountered in achieving stability with this entrance configuration, testing was planned with a partially contoured entrance with overlap.

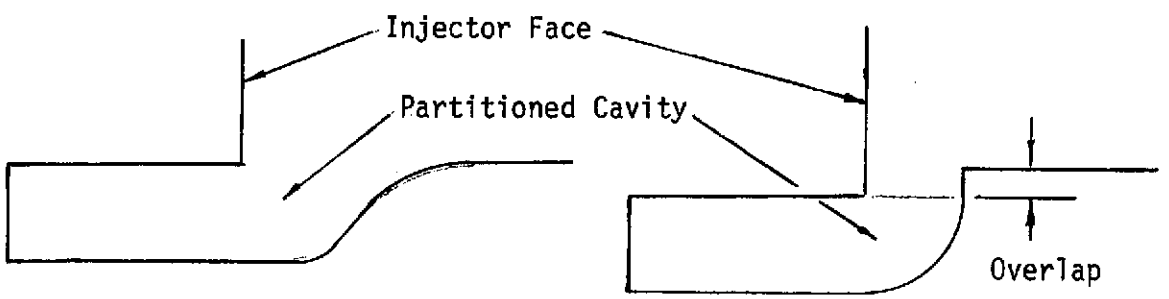


Contoured Entrance

Partially Contoured Entrance with Overlap

The partially contoured entrance was chosen as an alternative because Aerojet (Ref. 3) had found it necessary to use this alternative to stabilize their engine.

TABLE 1. SUMMARY OF STABILITY RESULTS FROM LOW CONTRACTION-RATIO CHAMBER TESTS

| Objective | Primary Cavity (1) $\sigma$ | Primary Cavity (2) $\ell_e$, in. | Secondary Cavity (1) $\sigma$ | Secondary Cavity (2) $\ell_e$, in. | $p_c$, psia | Overall Mixture Ratio | Fuel Inj. Temp., F | Maximum Damp Time, msec | Frequency, Hz | Stability |
|---|---|---|---|---|---|---|---|---|---|---|
| Stability of Basic Configuration | 0.148 | 1.60 | 0.074 | 0.78 | 130 | 1.80 | 180 | 14 | 2330 | Stable |
| | | | | | 126 | 1.71 | 190 | 220 | 2550 | Unstable |
| | | | | | 125 | 1.69 | 160 | 70 | 2570 | Unstable |
| | | | | | 140 | 1.55 | 165 | 11 | 2300 | Stable |
| | | | | | 113 | 1.52 | 165 | 11 | | |
| | | | | | 111 | 1.79 | 175 | 12 | | |
| Evaluate Effect of Manifold Dams | | | | | 137 | 1.52 | 175 | 12 | | Stable |
| | | | | | 123 | 1.66 | 160 | 13 | | |
| | | | | | 141 | 1.86 | 165 | 15 | | |
| | | | | | 111 | 1.42 | 150 | 14 | | |
| Stability with Reduced Open Area | 0.12 | 1.58 | 0.06 | 0.76 | 136 | 1.44 | 220 | 11 | | Stable |
| | | | | | 127 | 1.68 | 205 | 12 | 2770 | |
| | | | | | 140 | 1.80 | 195 | 70 | 2790 | Unstable |
| | | | | | 111 | 1.45 | 190 | 10 | | Stable |
| | | | | | 111 | 1.84 | 175 | 21 | 2790 | Marginal |
| | | | | | 127 | 1.61 | 175 | 10 | 2770 | Stable |
| | | | | | 143 | 1.65 | 170 | 18 | 2750 | |
| | | | | | 128 | 1.69 | 160 | 11 | 2800 | |

(1) $\sigma$ = fractional open area based on injector face area

(2) $\ell_e$ = effective cavity depth

The cavities for these tests were located in a single row around the injector face, 12 equal area cavities separated by partitions. Four equally spaced cavities were tuned to suppress the third-tangential and first-radial modes of instability. These cavities had an effective depth near 0.77 inch and a physical depth of 0.42 inch (measured from the injector face). The remaining eight cavities were tuned to suppress the first-tangential mode of instability and had effective and physical depths of ~1.59 and 1.25 inches, respectively. These effective depths were calculated from the acoustic model test results to be described below.

As shown in Table 1, two of the five tests with the initial cavity configuration were unstable (damp times exceeded 20 milliseconds) at a frequency of ~2560 Hz. A pressure record from one of these unstable tests is shown in Fig. 3. Based on initial analytical results this 2560 Hz mode of instability was thought to be, at least possibly, associated with the acoustics of the fuel injection system. Consequently, a modification to the injector was tried in which baffles (or dams) were installed at three locations with roughly equal spacing in the annular fuel manifold on the upstream side of the injector. With this modification, the combustion chamber was found to be stable. A pressure record from one of these tests is shown in Fig. 4. The remaining tests were made with a second cavity configuration having reduced open area. Two of the eight tests made with the latter configuration had damp times in excess of 20 milliseconds. Pressure records from one stable and one unstable test are shown in Fig. 5 and 6. This cavity configuration was inadequate to prevent a 2790 Hz oscillation. The analytical results to be discussed below suggest that this mode is also associated with the feed system.

HIGH CONTRACTION RATIO CHAMBER

For the second series of tests a 10-inch-diameter chamber, with a contraction ratio of 3.0 and injector-to-throat distances of 12 and 16 inches, was used. A new injector, L/D #4, designed for use in such a chamber, was used for these tests. This injector had 229 like-doublet elements (916 orifices) and no BLC injection. The fuel and oxidizer orifice diameters were 0.0294 and 0.0309 inches, respectively. A photograph of this injector and a cross-sectional schematic are shown in Fig. 7 and 8, respectively.

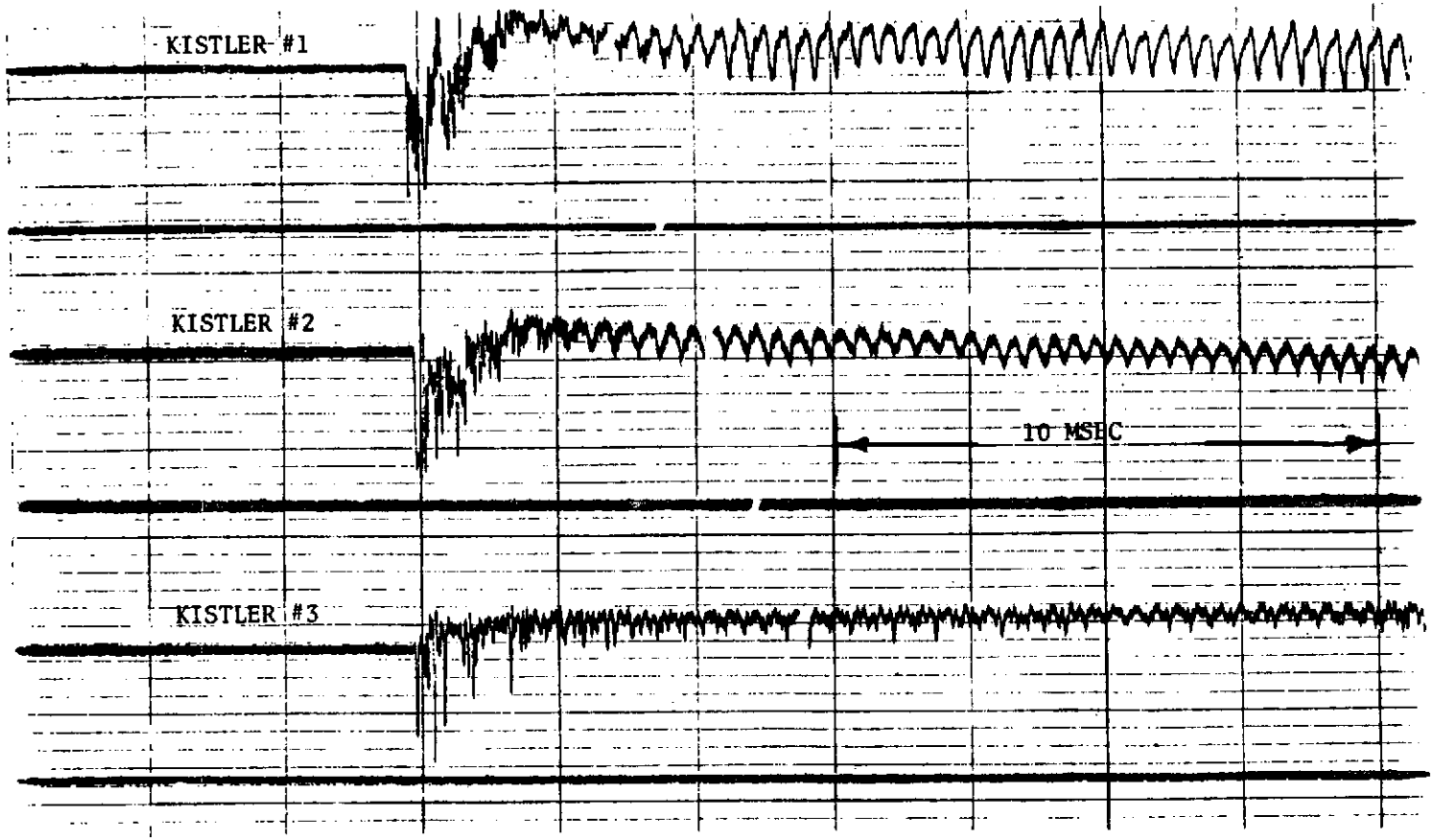


Test No. 3: First Bomb
Cavity: 0.148 x 1.60/0.074 x 0.78 (fraction x inch)
No Manifold Dams
Frequency: = 2570

FIGURE 3. HIGH FREQUENCY PRESSURE DATA

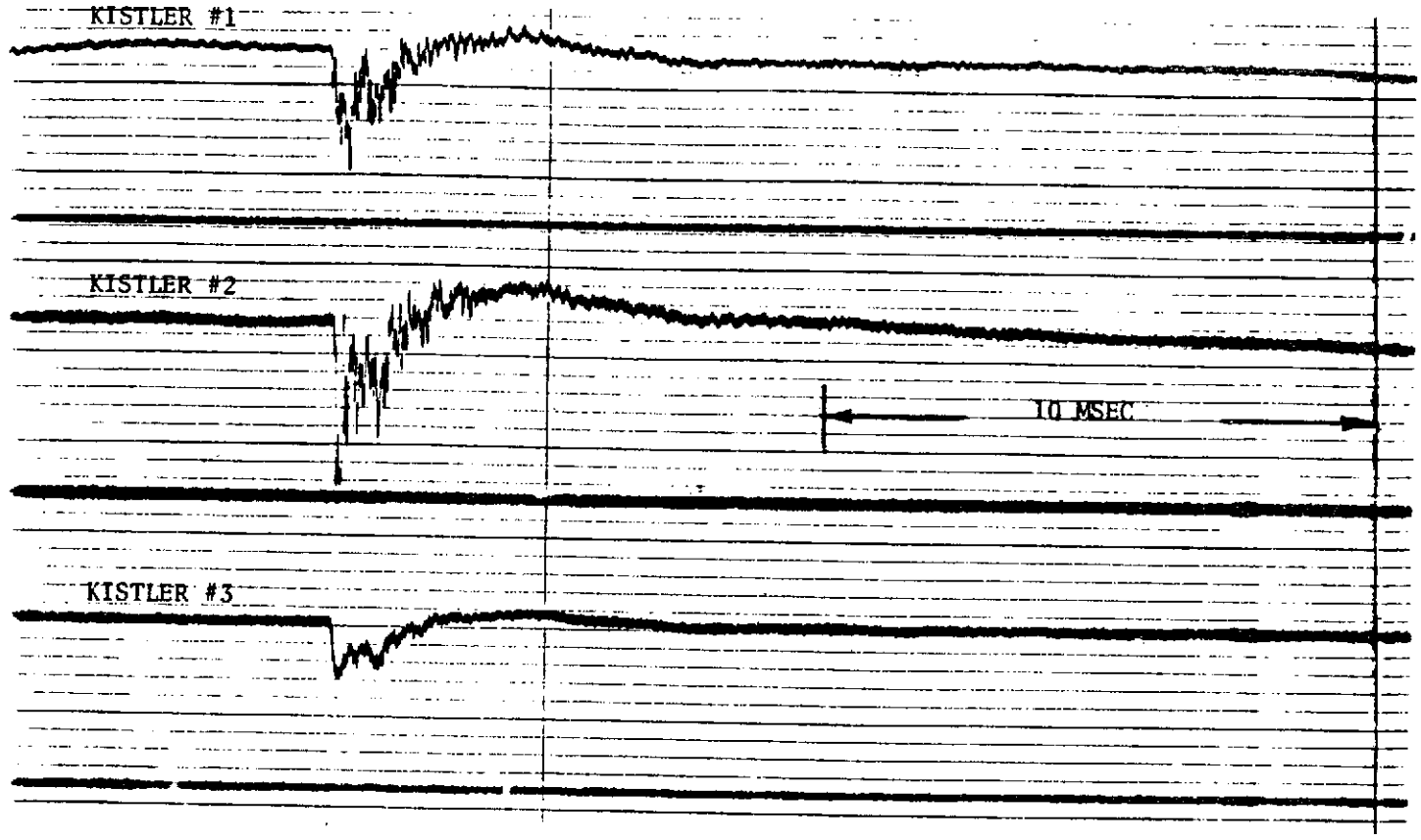


Test No. 8: First Bomb
Cavity: 0.148 x 1.60/0.074 x 0.78 (fraction x inch)
With Manifold Dams

FIGURE 4. HIGH FREQUENCY PRESSURE DATA

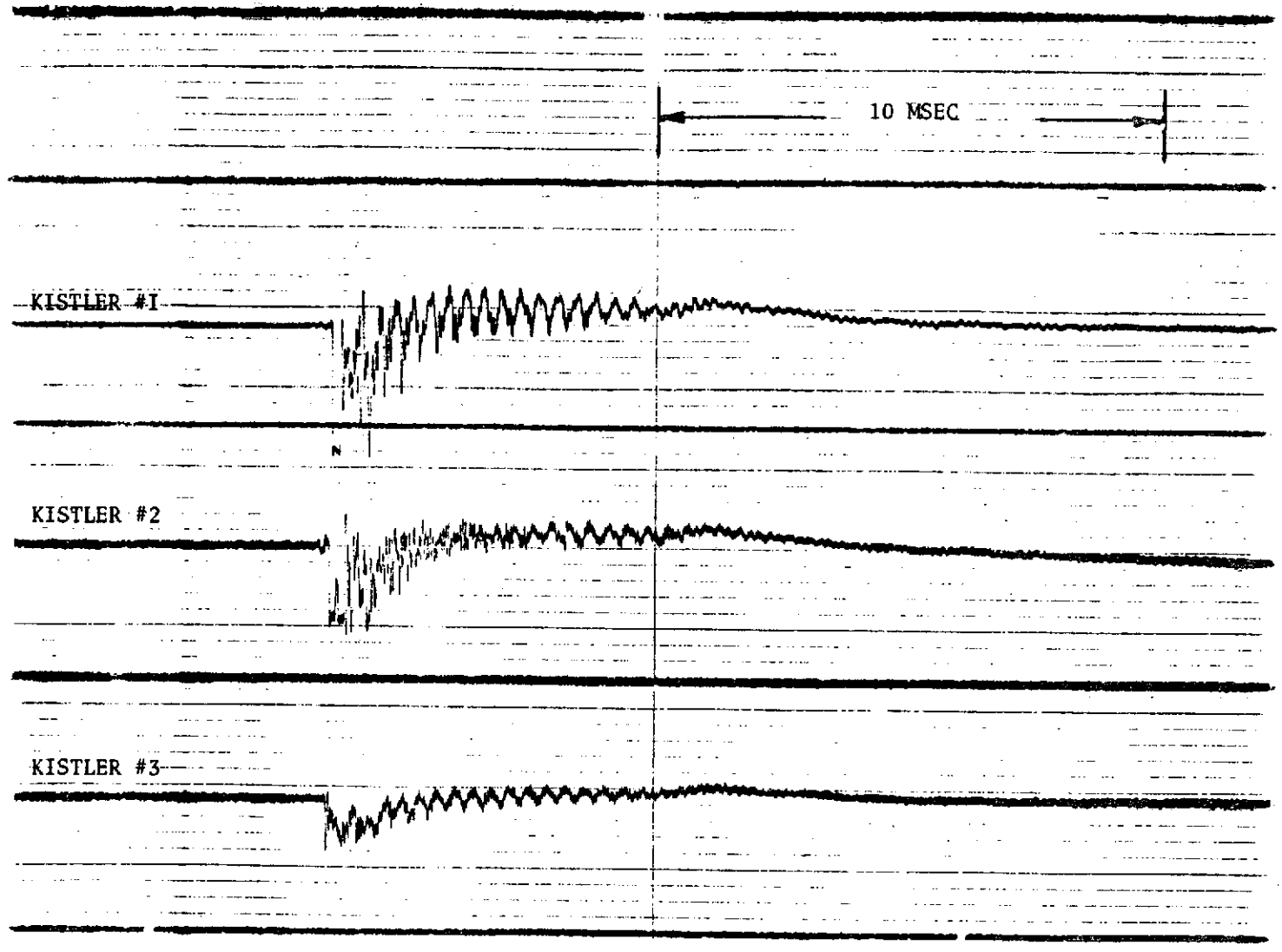


Test No. 12: Second Bomb
Cavity: 0.12 x 1.58/0.06 x 0.76 (fraction x inch)
Frequency = 2770 Hz

FIGURE 5. HIGH FREQUENCY PRESSURE DATA

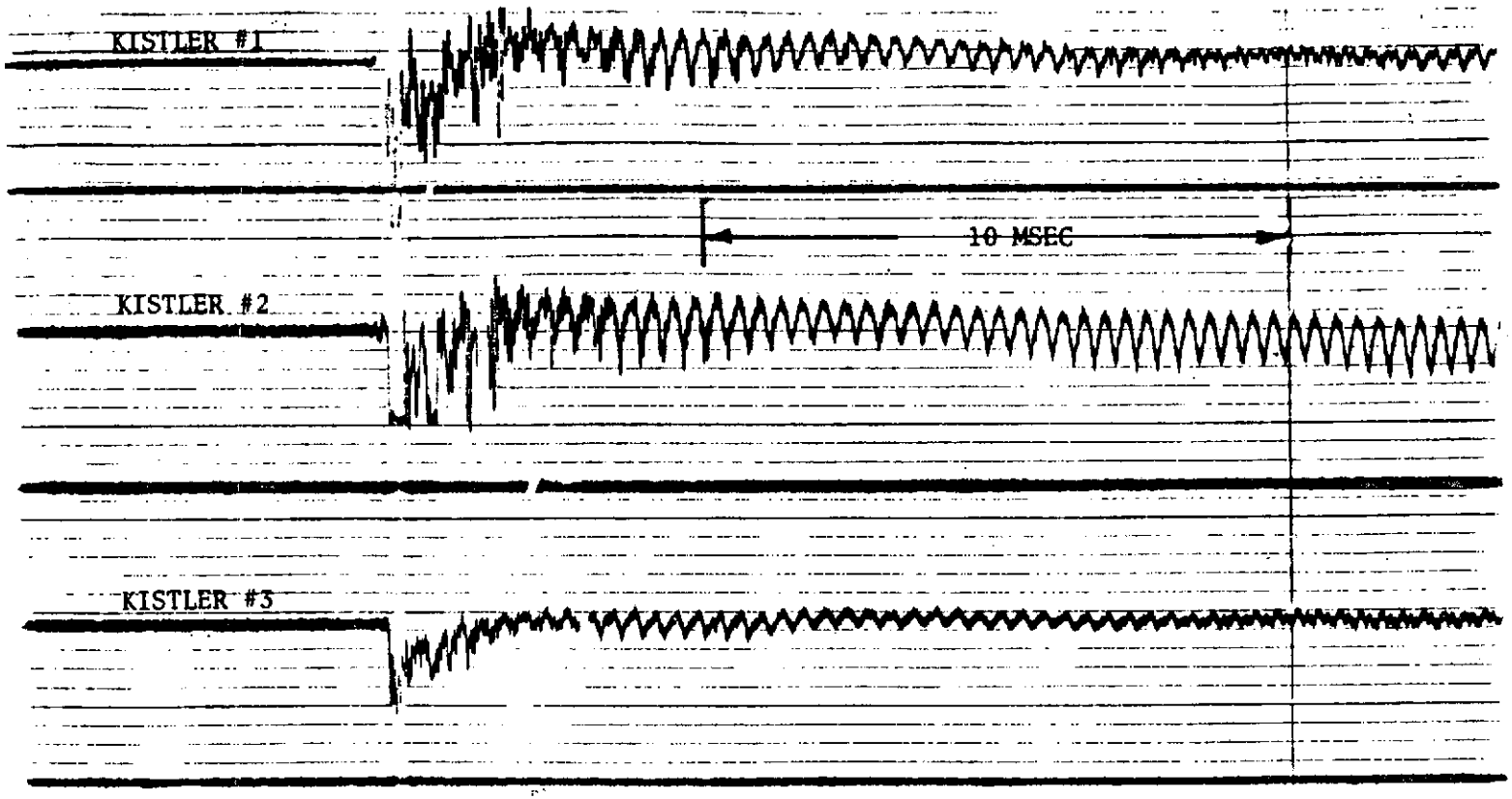


Test No. 13: First Bomb
Cavity: 0.12 x 1.58/0.06 x 0.76 (fraction x inch)
Frequency = 2790 Hz

FIGURE 6. HIGH FREQUENCY PRESSURE DATA

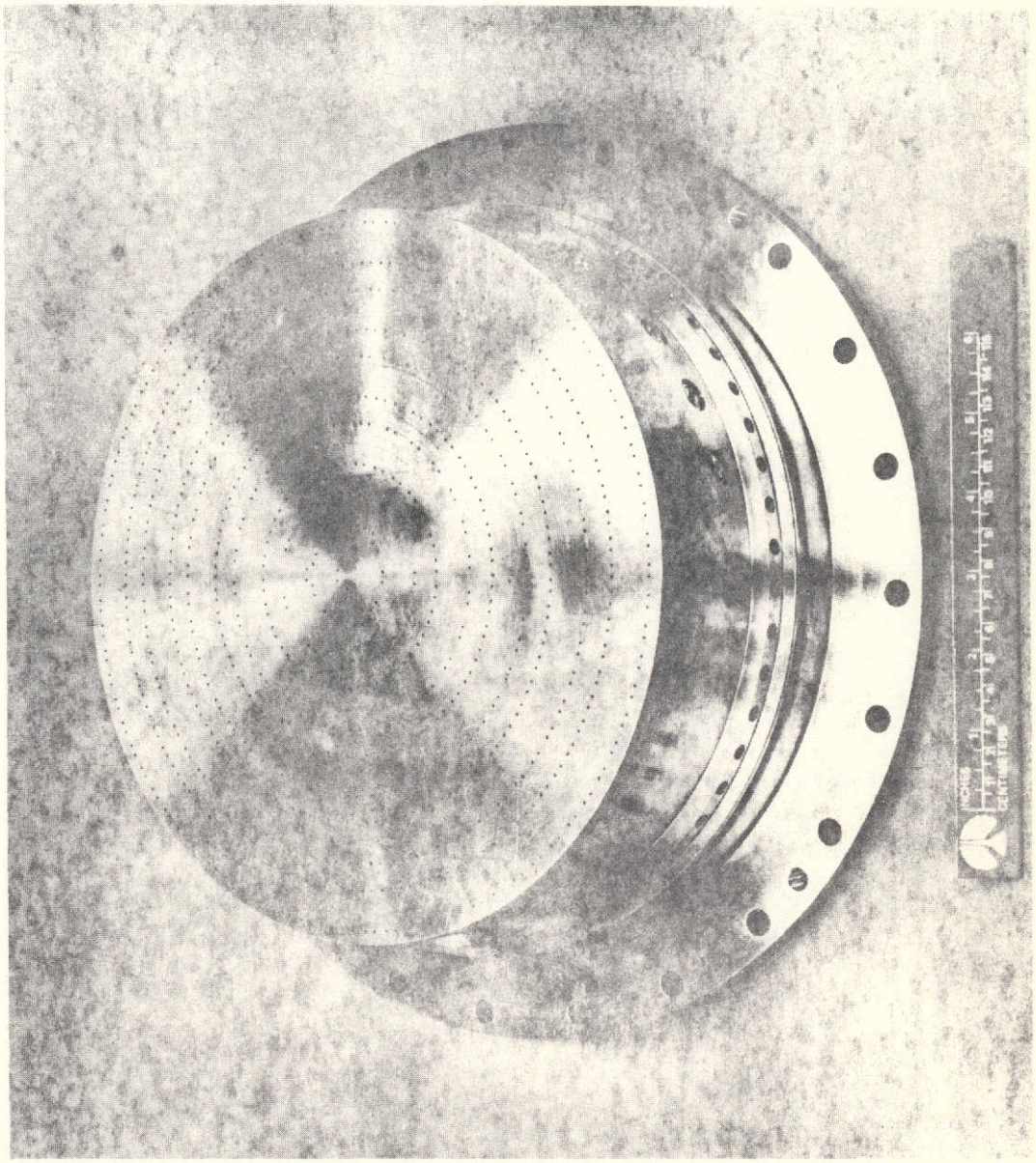

FIGURE 7. PHOTOGRAPH OF LIKE DOUBLET NO. 4 INJECTOR

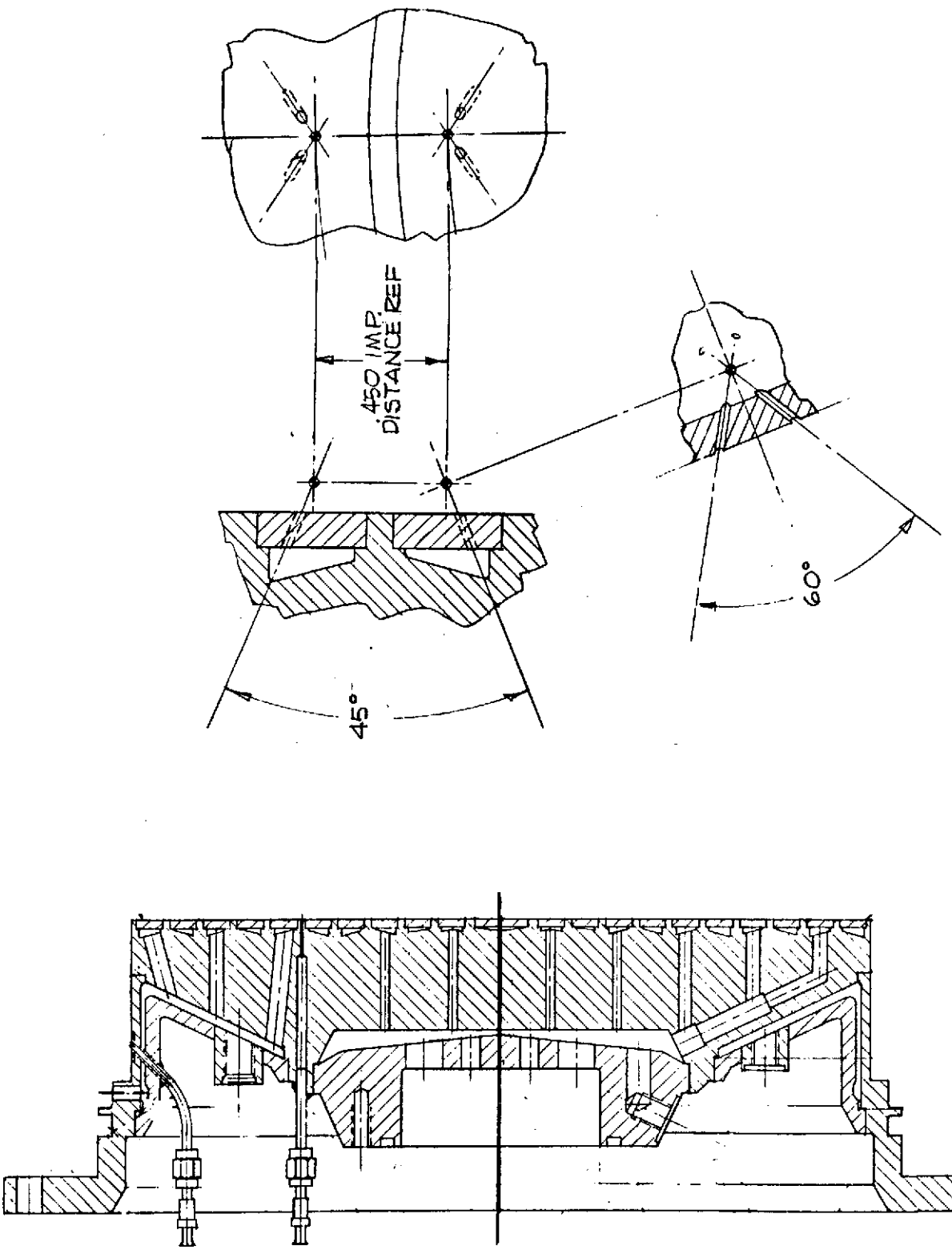


FIGURE 8. CROSS-SECTIONAL SCHEMATIC OF LIKE-DOUBLET NO. 4 INJECTOR

This chamber was instrumented in a manner similar to that used with the 8.2 inch diameter chamber. The high-frequency pressure transducers (Kistler Model 614B/644 or PCB Model 123A) and stability rating bombs were located 2.7 inches downstream from the injector face. The angular locations of the transducers were $12^{o}$, $108^{o}$, and $228^{o}$ from the fuel inlet. The bombs were located $60^{o}$ and $324^{o}$ from this inlet.

Stability results from testing the 10-inch-diameter chamber are summarized in Table 2. Each entry in the table corresponds to a single test with two bombs being used for each test, nominally. The cavity configurations were similar to those used in the 8.2-inch-diameter chamber with contoured entrances and with 4 of 12 cavities tuned for the third-tangential and first-radial modes and 8 of 12 cavities tuned for the first tangential mode. The effective and physical depths of the secondary (3T/1R) cavity was 0.88 and 0.5 inches, respectively, for all tests. Testing was initiated with a 9.9 percent open area primary (1T) cavity (with effective and physical depths of 2.08 and 1.75 inches, respectively), which proved adequate to prevent instability. However, a shallow 14.8 percent open area cavity was found to be inadequate. The latter cavity had an effective depth of 1.28 inches and a physical depth of 0.9 inch. Nevertheless, subsequent testing with a deeper 14.8 percent open-area cavity showed it to be adequate (physical depth of 1.75 inches).

The remaining tests were made, primarily, to evaluate the effects of fuel temperature and chamber length on steady-state performance, because the performance was less than anticipated. However, the combustion chamber was stable during all remaining tests.

## SUMMARY OF RESULTS FROM FULL-SCALE TESTING

Results from testing the 8.2-inch-diameter (low contraction ratio) chamber show that:

1. Stability was readily achieved with a contoured entrance cavity without overlap.

TABLE 2. SUMMARY OF STABILITY RESULTS FROM HIGH CONTRACTION-RATIO CHAMBER TESTS

| Objective | Primary Cavity (1) σ | Primary Cavity (2) $\ell_e$, in. | Secondary Cavity (1) σ | Secondary Cavity (2) $\ell_e$, in. | $p_c$, psia | Overall Mixture Ratio | Fuel Inj. Temp., F | Maximum Damp Time, msec | Frequency, Hz | Stability |
|---|---|---|---|---|---|---|---|---|---|---|
| Search for Minimum Open Area ↓ | 0.099 ↓ | 2.08 ↓ | 0.069 ↓ | 0.88 ↓ | 120 | 1.64 | 190 | 7 | | Stable ↓ |
| | | | | | 134 | 1.84 | 220 | 7 | | |
| | | | | | 136 | 1.54 | 210 | 6 | | |
| | | | | | 118 | 1.73 | 160 | 9 | | |
| Search for Minimum Depth ↓ | 0.148 ↓ | 1.28 ↓ | | | 127 | 1.66 | 190 | 570 | 2640 | Unstable |
| Confirm Stability at Nominal Depth ↓ | 0.148 ↓ | 2.12 ↓ | | | 126 | 1.66 | 201 | 6 | | Stable ↓ |
| | | | | | 140 | 1.80 | 192 | 6 | | |
| | | | | | 132 | 1.44 | 188 | 6 | | |
| | | | | | 114 | 1.82 | 189 | 7 | | |
| | | | | | 126 | 1.62 | 190 | 6 | | |
| | | | | | 140 | 1.61 | 185 | 5 | | |
| | | | | | 110 | 1.48 | 176 | 7 | | |
| | | | | | 126 | 1.67 | 187 | 8 | | |
| | | | | | - | - | - | 8 | | |
| | | | | | 125 | 1.62 | 70 | 8 | | |
| | | | | | 139 | 1.86 | 68 | 7 | | |
| Confirm Stability with Long Chamber ↓ | 0.099 ↓ | 2.08 ↓ | | | 129 | 1.42 | 65 | 7 | | |
| | | | | | 125 | 1.69 | 225 | 8 | | |
| | | | | | 140 | 1.86 | 200 | 7 | | |
| | | | | | 140 | 1.54 | 194 | 7 | | |
| | | | | | 112 | 1.88 | 183 | 8 | | |
| | | | | | 112 | 1.71 | 194 | 8 | | |
| | | | | | 126 | 1.66 | 183 | 8 | | |

(1) σ = Fractional open area based on injector face area.

(2) $\ell_e$ = Effective cavity depth.

2. Stability was dominated by 2300 to 2800 Hz oscillation and which was improved by installing baffles (dams) in the fuel manifold.

3. The change in BLC introduction from a separate downstream injector to the periphery of the main injector did not significantly affect stability. Moreover, the stability of the L/D #1 injector appeared comparable but slightly better than that of the L/D #2 injector (described in Ref. 2).

Results from testing the 10-inch-diameter (high contraction ratio) chamber show that:

1. Adequate stability was readily achieved with a contoured entrance cavity without overlap.

2. The L/D #4 injector is relatively stable. Because the performance was somewhat low, the greater stability may not be due to the higher contraction ratio.

## ACOUSTIC MODEL TESTING

Two kinds of acoustic model tests were made, one with relatively detailed models of the acoustic cavities only and the second with a model of the combustion chamber containing acoustic cavities. The tests with the detailed cavity models were made to measure the effective acoustic depth of these cavities associated with the entrance region. The tests with the chamber model were made to measure the influence of the cavities on the acoustic modes of the chamber. Each kind of model was excited with an acoustic driver and the model response was measured with a microphone. The frequencies corresponding to maximum microphone response were interpreted as the resonant frequencies of the models.

### CAVITY MODEL TESTING

The general configuration of the cavity models is illustrated in Fig. 9. The model was constructed from Lucite as a three-times scale two-dimensional representation of the cavity configurations of interest. Replaceable entrance block configurations were used to model the different cavity configurations. The entrance to the cavity model was exposed to the room and was not contained in another chamber. As finally used, the model was enclosed on one side only to the level of the surface corresponding to the combustion chamber wall. Originally, the model was designed for use with two relatively large sheets which would restrict the flow in the entrance region to two-dimensions. However, these sheets formed a rectangular cavity which was open on two sides and which behaved as a resonator itself. The resonant frequencies of this larger cavity dominated those exhibited by the acoustic cavity model being tested and prevented adequate measurements.

The resonant characteristics of the cavity models were determined by measuring the variation in resonant frequency as the cavity depth was varied by moving the piston, with the various entrance configurations.

Results from these model tests are shown in Fig. 10 through 12. The results are shown as an effective depth, which is simply the calculated

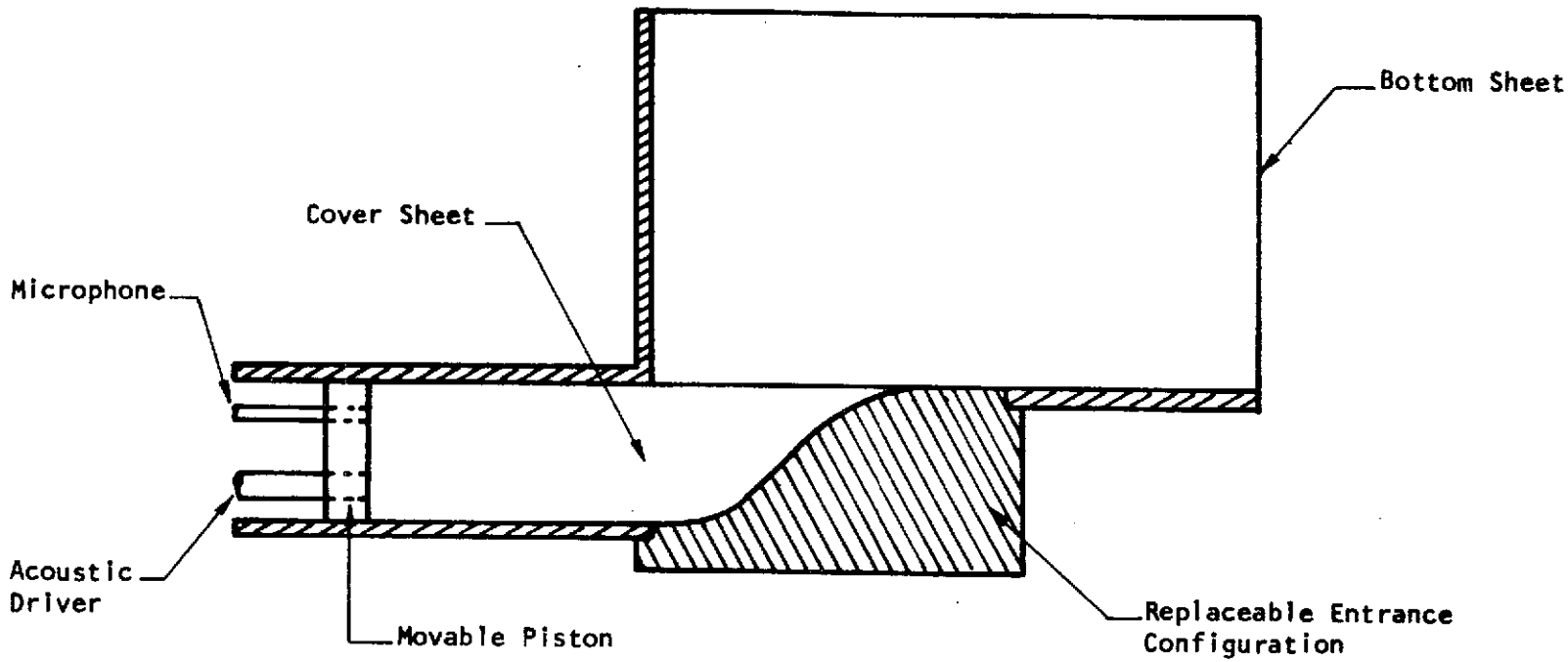


FIGURE 9. SCHEMATIC DIAGRAM OF ACOUSTIC CAVITY MODELS

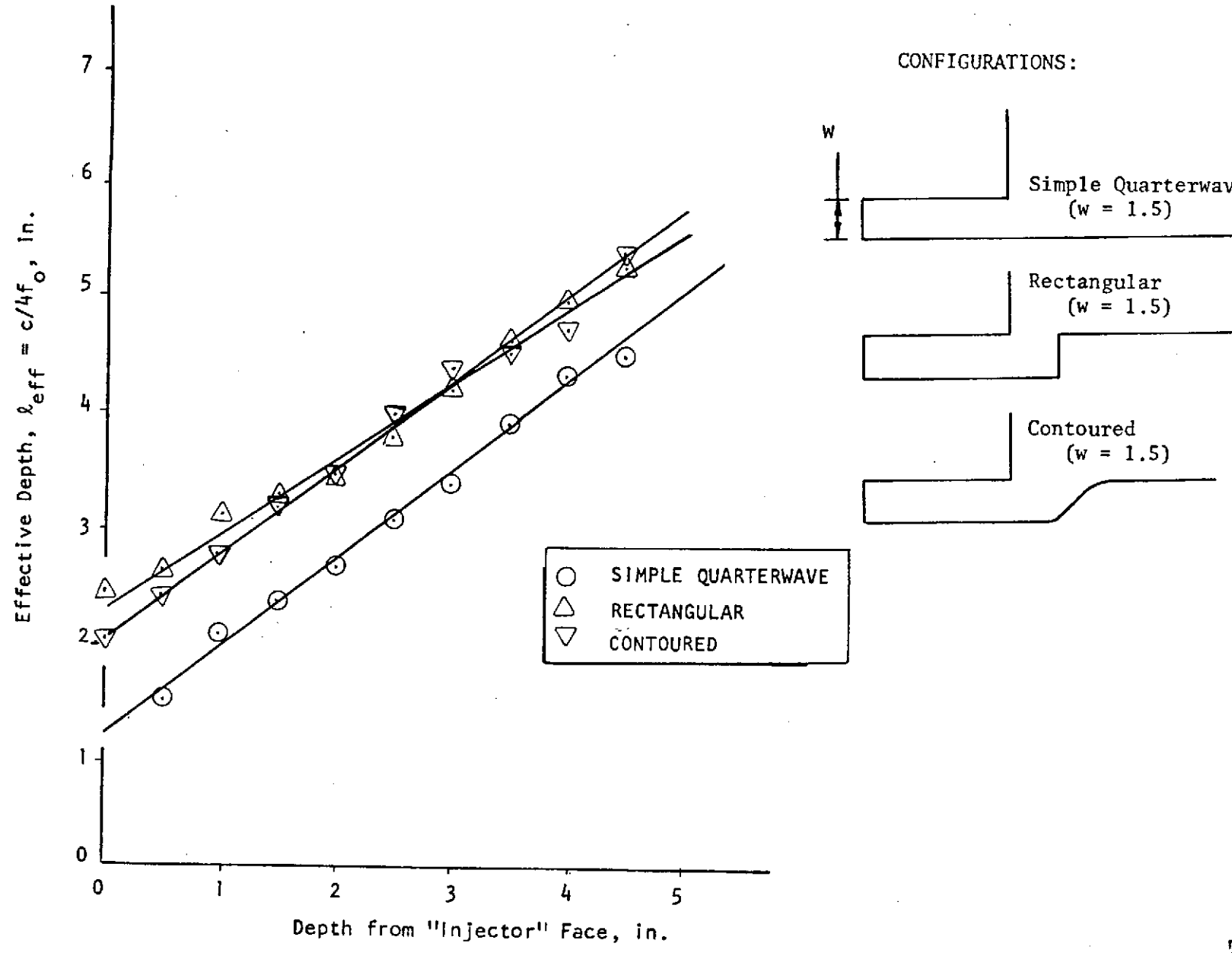


FIGURE 10. ACOUSTIC MODEL TEST RESULTS

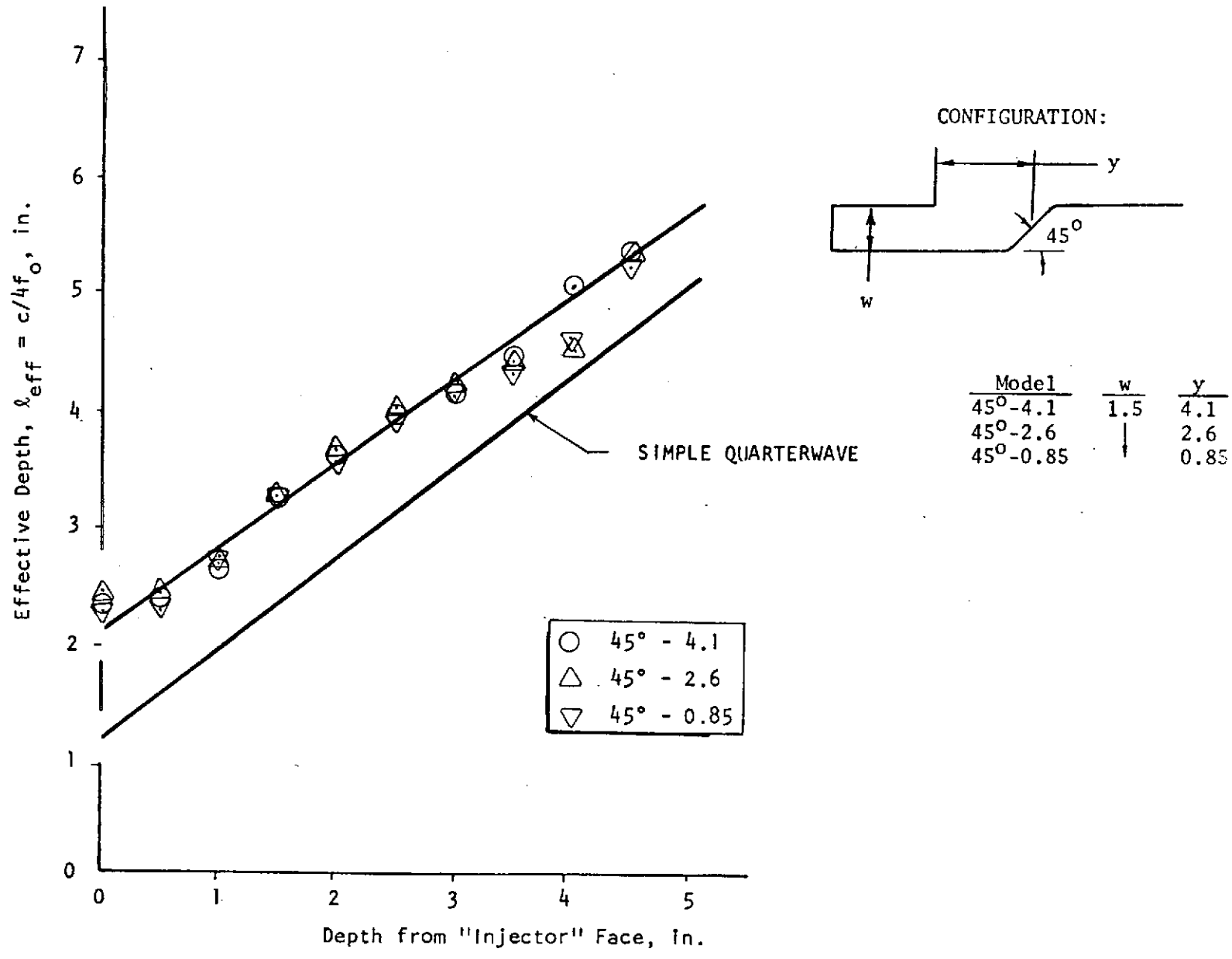


FIGURE 11. ACOUSTIC MODEL TEST RESULTS

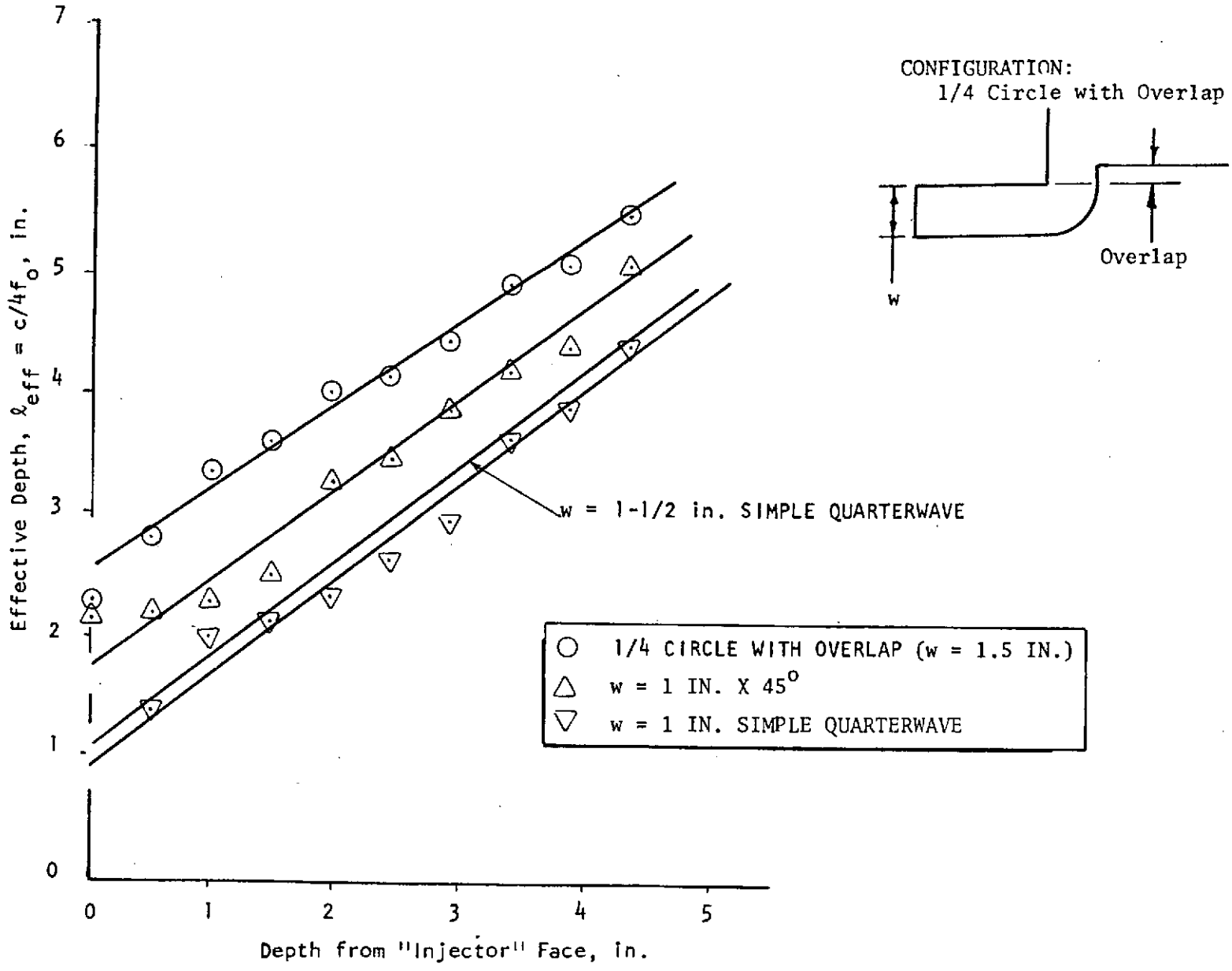


FIGURE 12. ACOUSTIC MODEL TEST RESULTS

quarterwave depth corresponding to the measured resonant frequency, as a function of physical depth. The various cavity configurations are illustrated in each figure as well. The primary purpose of these tests was to determine the effective depth contribution resulting from the entrance region of the cavity. This depth contribution was calculated from the test results as the horizontal distance between the line for the cavity of interest and the line for a simple quarterwave resonator with the same cavity width (open area).

Because the test results appear to fall along straight lines, the depth contribution from the entrance region is also a linear function of depth, i.e.,

$$\delta = a - bz$$

calculated values for each of these parameters, scaled by the 3:1 factor used in constructing the models, (a and b) from the test results are shown in Table 3.

TABLE 3. EFFECTIVE DEPTH PARAMETERS FROM MODEL TEST RESULTS (SCALED TO CHAMBER SIZE BY 3:1)

| Resonator Model | a (in.) | b (in./in.) | w (in.) |
|---|---|---|---|
| 1 in./45° | .36 | 0.0175 | 0.33 |
| 1½ in./45° (3 configurations) | .40 | 0.0275 | 0.50 |
| ¼ circle W/O.L. | .65 | 0.040 | |
| Contoured | .37 | 0.013 | |
| Rectangular | .47 | 0.050 | |

Employing the results from the 1 in./45° and 1½ in./45° results, the following equation for any width was obtained:

$$\delta \simeq a(0.6w + 0.7) - bz(2.18w - 0.091)$$

Two significant observations may be made from the test results. First, the results shown in Fig. 11 indicate the resonant frequency of the resonator is substantially unaffected by the position of the downstream portion of the cavity entrance, when varied over a range of 0.6 to 2.7 times the cavity width. Secondly, the overlap (0.2 inch) used with ¼ circle entrance (similar to Aerojet partial contours) has apparently increased the effective depth by an amount approximately equal to the overlap; a conclusion inferred from comparison with the results for the rectangular entrance.

## CHAMBER MODEL TESTING

A model of the combustion chamber containing acoustic cavities was also constructed. This model is shown schematically in Fig. 13. It was constructed from three concentric ¼-inch-wall Lucite tubes to form a chamber and six variable depth cavities. The depth of the rectangular entrance cavities could be varied individually with sliding pistons which closed the cavities. The pistons were sealed (against acoustic pressures) by coating them with petroleum jelly and by narrow strips of Teflon used as sliding seals along the radial surfaces of each piston. The microphone and acoustic driver were connected through the chamber wall near the acoustic cavity. A wire-filled coupling tube was used to isolate the driver acoustically from the model.

Employing this model, the variation of the resonant frequency of the lowest nine chamber modes with varying cavity depth was measured. The results are shown in Fig. 14, where the circular symbols correspond to measured frequencies (frequencies corresponding to response maxima). The curves in Fig. 14 correspond to predicted frequencies for each of the indicated modes. Generally, the predicted and measured frequencies agree very well. This comparison will be discussed further below in connection with the description of the analytical studies.

## SUMMARY OF ACOUSTIC MODELING RESULTS

Results from the acoustic model tests with the detailed cavity models has allowed determination of the effective depth contribution from a relatively wide range of cavity configurations. Moreover, the results indicate the effective depths are surprisingly insensitive to variation in entrance configuration, especially the location of the downstream portion of the cavity entrance.

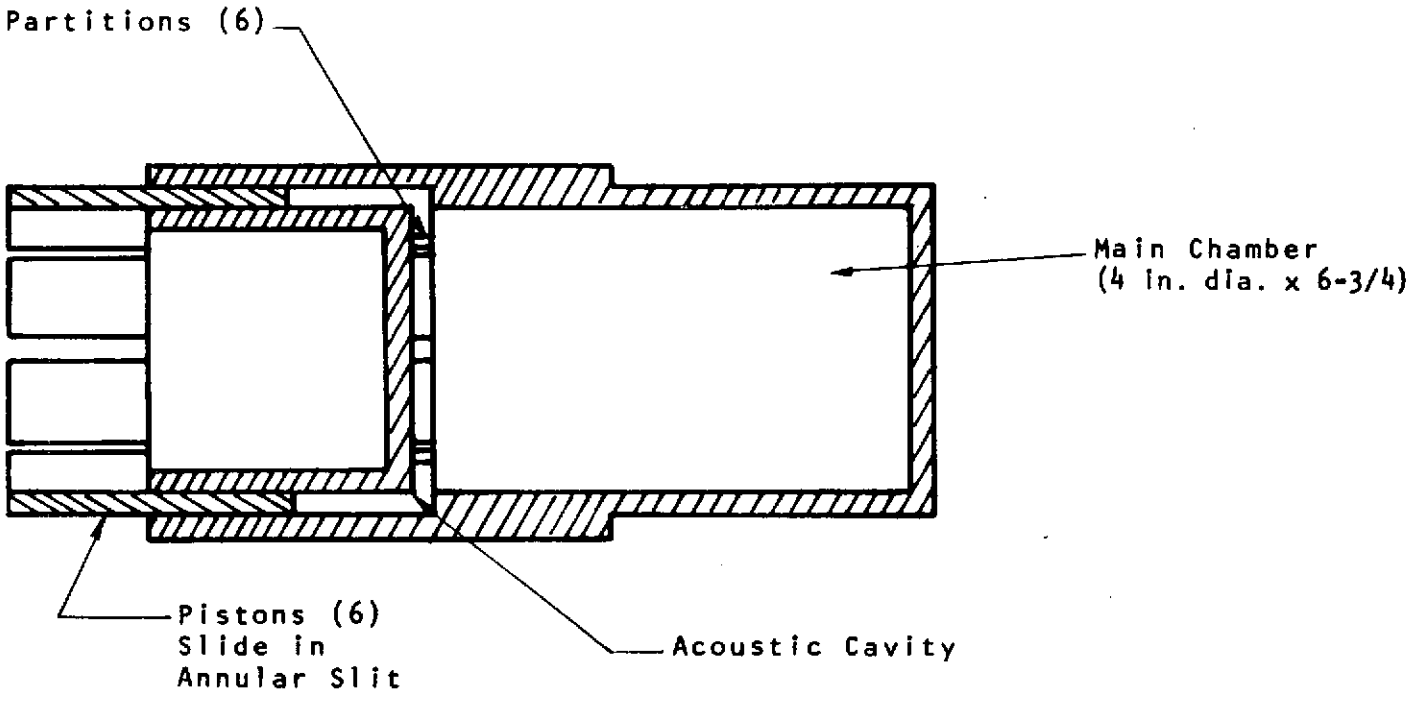


FIGURE 13. SCHEMATIC DIAGRAM OF CHAMBER ACOUSTIC MODEL

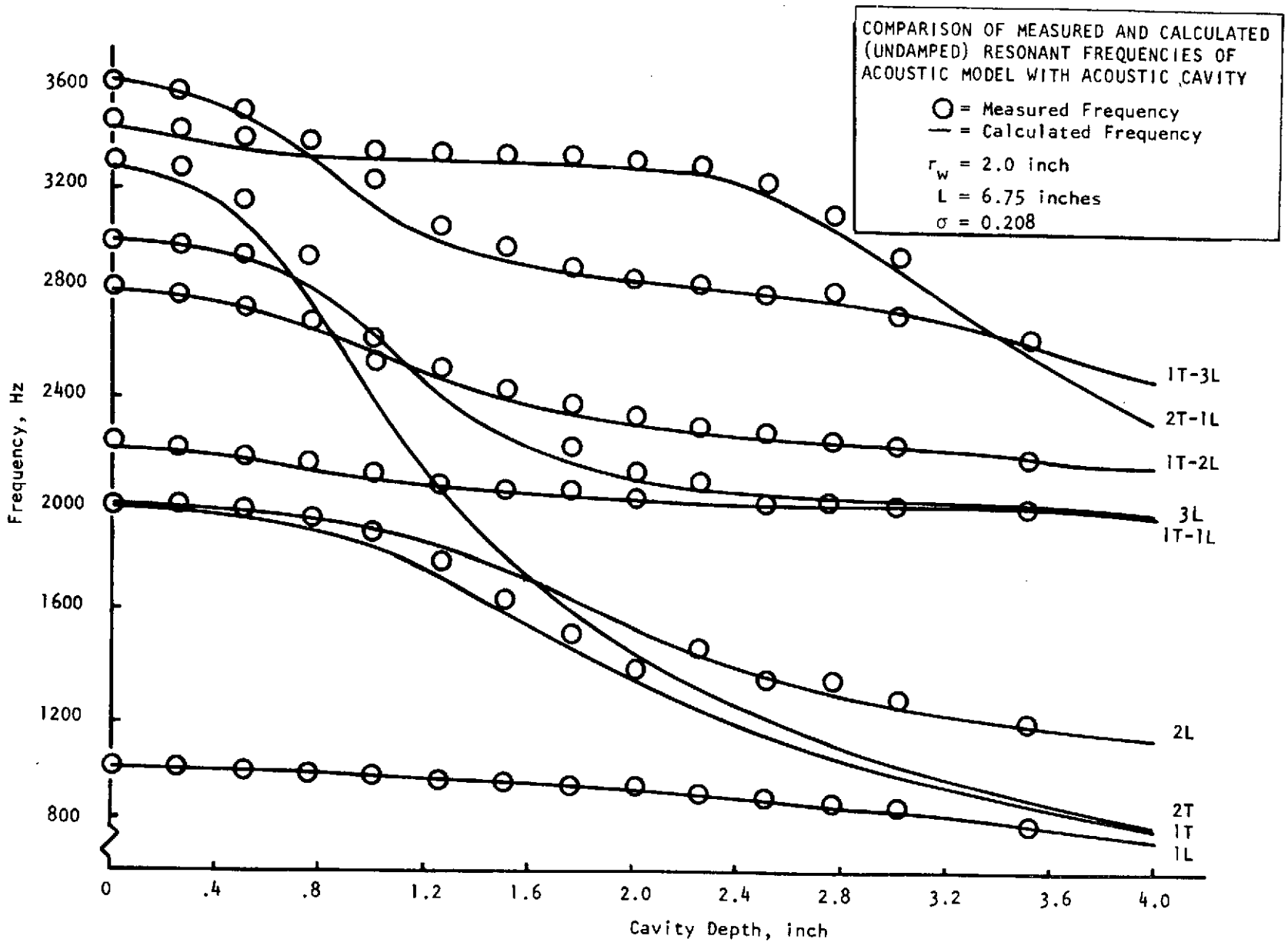


FIGURE 14. RESULTS FROM TESTING CHAMBER ACOUSTIC MODEL

# ANALYSIS AND INTERPRETATION OF TEST RESULTS

The purposes of the analytical effort under this program were to aid design of the cavities to be tested and to aid evaluation, from the available data, of the effectiveness of acoustic cavities for suppressing instabilities. Most of the effort was directed toward assessing the significance of the 2300 to 2800 Hz oscillation experienced during testing on this and other programs.

The 2300 to 2800 Hz oscillation has been encountered repeatedly during testing of 8-inch-diameter chambers at Rocketdyne and Aerojet (Ref. 2 and 3). Rocketdyne has interpreted this oscillation as not being due to a normal chamber mode and probably associated with the acoustics of the feed system. With this interpretation the acoustic cavity would be expected to weakly affect stability. Conversely, Aerojet has interpreted the oscillation as being due to the first tangential mode of the chamber with its frequency being suppressed by the acoustic cavity. Aerojet has tried many cavity configurations in an effort to suppress the oscillation.

This oscillation has significant implications relative to cavity effectiveness if the chamber mode interpretation is correct because the oscillation has been quite resistant to suppression, although some small changes in cavity configuration have substantially affected stability. Conversely, if the feed system interpretation is correct, solutions to the problem should be sought in the injector and feed system rather than by modifying the cavity.

In an effort to identify the mode or modes and clarify the implications relative to cavity effectiveness, analytical studies were made of both of these possibilities.

OBSERVATIONS CONCERNING 2300 TO 2600 HZ OSCILLATION

Considerable testing has been done at Rocketdyne and Aerojet with 8-inch-diameter chambers. The expected frequencies of oscillations may be estimated in the usual manner from the acoustic equations for a closed chamber. For the chamber used during this program, the estimated chamber mode frequencies are:

Table 4. Expected Frequencies in Rocketdyne Chamber with no Cavities

| Mode[1] | Frequency (Hz)[2] |
|---|---|
| 1L | 1631 |
| 2L | 3262 |
| 1T | 3194 |
| 1T-1L | 3586 |
| 2T | 5298 |
| 1R | 6647 |
| 3T | 7288 |

[1] 1L, 1T, 1R, ... denote the first longitudinal, first tangential, first radial, ... modes.

[2] Sound velocity: 3724 ft/sec (95 percent of theoretical shifting)

The expected frequencies for the Aerojet chamber would differ slightly from this. Thus, the expected frequency for the first tangential mode would be ~3200 Hz. The acoustic cavity would be expected to reduce this somewhat.

A frequency in this range was encountered during testing at Rocketdyne with an unlike doublet injector (8.2-inch-diameter chamber) but no 2600 Hz oscillation. Oscillation was observed in the range of 3000 to 3100 Hz, some higher frequencies and some in the range 480 to 1030.

During testing at Rocketdyne with the L/D #2 injector, multiple instances of 2380 to 2640 Hz oscillation were observed. This oscillation usually appeared during the damping of a bomb induced transient. It always occurred with a nominal fuel temperature of 200°F (no instances with 250°F fuel) and with a primary cavity open area fraction of 16 to 22 percent. With a smaller open area (13 percent) a 3000 Hz oscillation appeared.

During Rocketdyne testing with the L/D #1 injector, multiple instances of 2300 to 2800 Hz oscillation have been observed. However, dams in the fuel manifold eliminated the oscillation with 14.8 percent open area cavity. When the modified injector was tested in a 12 percent open area cavity, the frequency shifted to 2790 Hz from the 2560 Hz which had occurred earlier.

Aerojet has done extensive testing with an 8.1-inch-diameter chamber. With platelet injectors, 2300 to 2900 Hz oscillation has occurred with a wide range of cavity configurations. Moreover, when the cavity was blocked 5200 and 6400 Hz oscillations occurred. During this testing the contour of the cavity entrance and the amount of cavity overlap strongly influenced the instability.

Aerojet tests with a conventional like-doublet injector exhibited 2800 Hz oscillation with a shallow cavity and 3200 Hz with the cavity blocked off.

Bell (Ref. 4) has not reported testing an 8-inch chamber but has done extensive testing with a 10-inch-diameter chamber. In this chamber 2520 to 2620 Hz oscillation was observed with a small open area 1T mode cavity, which corresponds to 3070 to 3200 Hz in an 8.2-inch-diameter chamber.

These results suggest that when the cavity open area is insufficient, oscillation near the expected normal mode frequencies will occur, i.e., ~3000 to 3100 Hz which appears to be the first tangential mode with a slightly depressed frequency (the Aerojet platelet appeared to exhibit

the second tangential and first radial modes). However, with larger open area cavities the 2300 to 2900 Hz oscillations appear with the like-doublet injectors in 8-inch-diameter chambers. If these lower frequencies correspond to a first-tangential mode with a depressed frequency, the frequency reduction is as much as 28 percent.

## ANALYSIS OF THE EFFECTS OF CAVITIES ON CHAMBER MODE FREQUENCIES

In an effort to assess the likelihood of the 2300 to 2900 Hz behavior being entirely or partially due to the acoustic cavities, the effects of cavities on the chamber modes were analyzed. The Rocketdyne analytical model (Ref. 2) for predicting the damping effects of acoustic cavities was used for this purpose. The validity of model predicted frequency effects was confirmed by comparison with acoustic model test results. Further, a new variation of the model was used, which accurately describes the alternating cavity arrangement being used. An approximation was necessary with the model as previously used.

A comparison between predicted and measured frequencies for the chamber acoustic model tests was shown in Fig.14. Based on this comparison, the model is believed to accurately predict the cavity effects. The observed variations are generally predicted very well, although in some regions a mode is predicted but not observed and in other regions only one frequency was measured and several are predicted. However, these inaccuracies may be attributed to the measurement technique. In regions where multiple modes are predicted and only one frequency is observed, the measurement technique is such that the responses of all near resonant modes is likely to merge to give a single response peak. In regions where modes are predicted and none observed, the modes are likely to be highly damped and not apparent with the measurement technique. Thus, use of the model to predict frequency effects in the hot chamber case appears fully justified.

Predicted frequency variations for the first-tangential and second-longitudinal modes in the Rocketdyne 8.2-inch-diameter chamber are shown in Fig. 15.

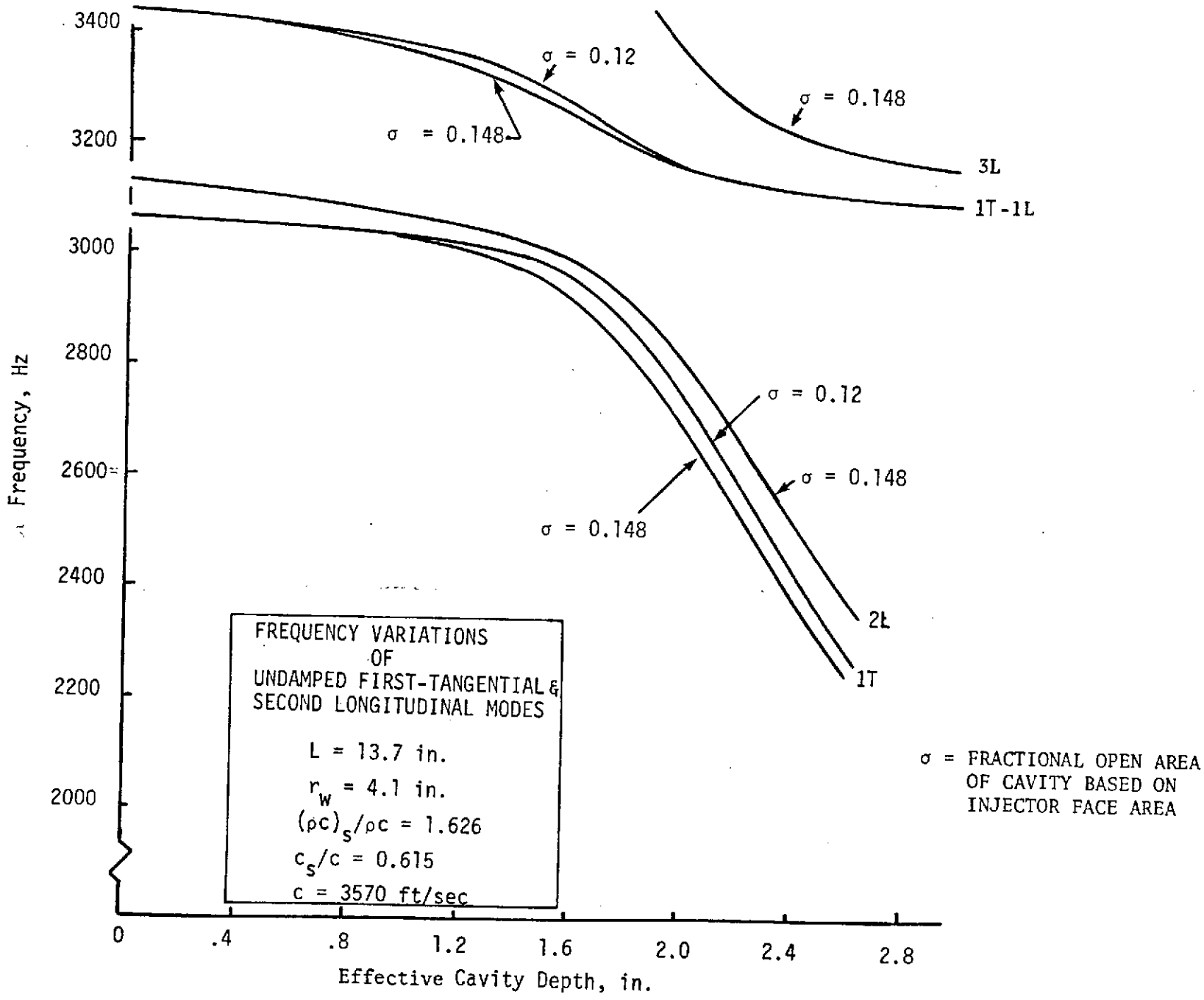


FIGURE 15. PREDICTED FREQUENCY VARIATIONS WITH CAVITY DEPTH

(a somewhat lower sound velocity was used for these calculations, which was based on measured frequencies obtained with narrow cavities, than was used for Table 4). These calculations show that a 2300 to 2900 Hz first-tangential mode frequency is possible, but the frequency of the first-tangential-first-longitudinal is near 3100 Hz under the same conditions. Moreover, relatively deep cavities are required (or lower sound velocities in the cavities) and the frequency should decrease with increasing cavity depth at ~800 Hz/inch. A sound velocity error ~25 to 30 percent is needed to account for the difference in predicted and actual depths. Also, the actual frequency change with increased depth is ~200 Hz/inch. In addition, a frequency change of ~50 Hz would be expected when the cavity fractional open area is increased from 0.148 to 0.12. The actual change was ~200 Hz. The disparity between the actual and predicted is too large to appear likely.

A related set of calculated results is shown in Fig. 16, which show predicted cavity damping for the first tangential and first-tangential-first-longitudinal modes. The curves denoted as circumferentially uniform and nonuniform were obtained with the original cavity damping model and the new variation of the model, respectively. Clearly, there is little difference for this case between calculations, indicating the alternating cavity arrangements used for the full-scale tests does not cause unexpected behavior. The set of points in this figure denoted by various values of $\ell_2$ correspond to predicted damping for the indicated values of secondary cavity depth.

Also shown in Fig. 16 is the cavity depth corresponding to a depressed first-tangential mode frequency of 2600 Hz. At this depth the first-tangential (1T) mode is very highly damped (the actual level is not shown but appears to be ~3000 $sec^{-1}$) whereas the first-tangential-first-longitudinal (1T-1L) mode has a damping coefficient of 310 $sec^{-1}$ and a frequency of 3100 Hz. Thus, it seems unlikely that the 1T mode would be excited more readily than the 1T-1L mode with an order of magnitude less damping and a frequency near that of the normal 1T mode without a cavity.

Figure 18 shows the variation of predicted damping with cavity depth for various values of the amplitude parameter $\Gamma\hat{p}/\gamma p$. The curves for $\Gamma\hat{p}/\gamma p_o = 0.0$ correspond to the undamped case shown previously in Fig. 15. Thus, as damping is introduced it becomes more unlikely that a frequency of ~2600 Hz could be reached.

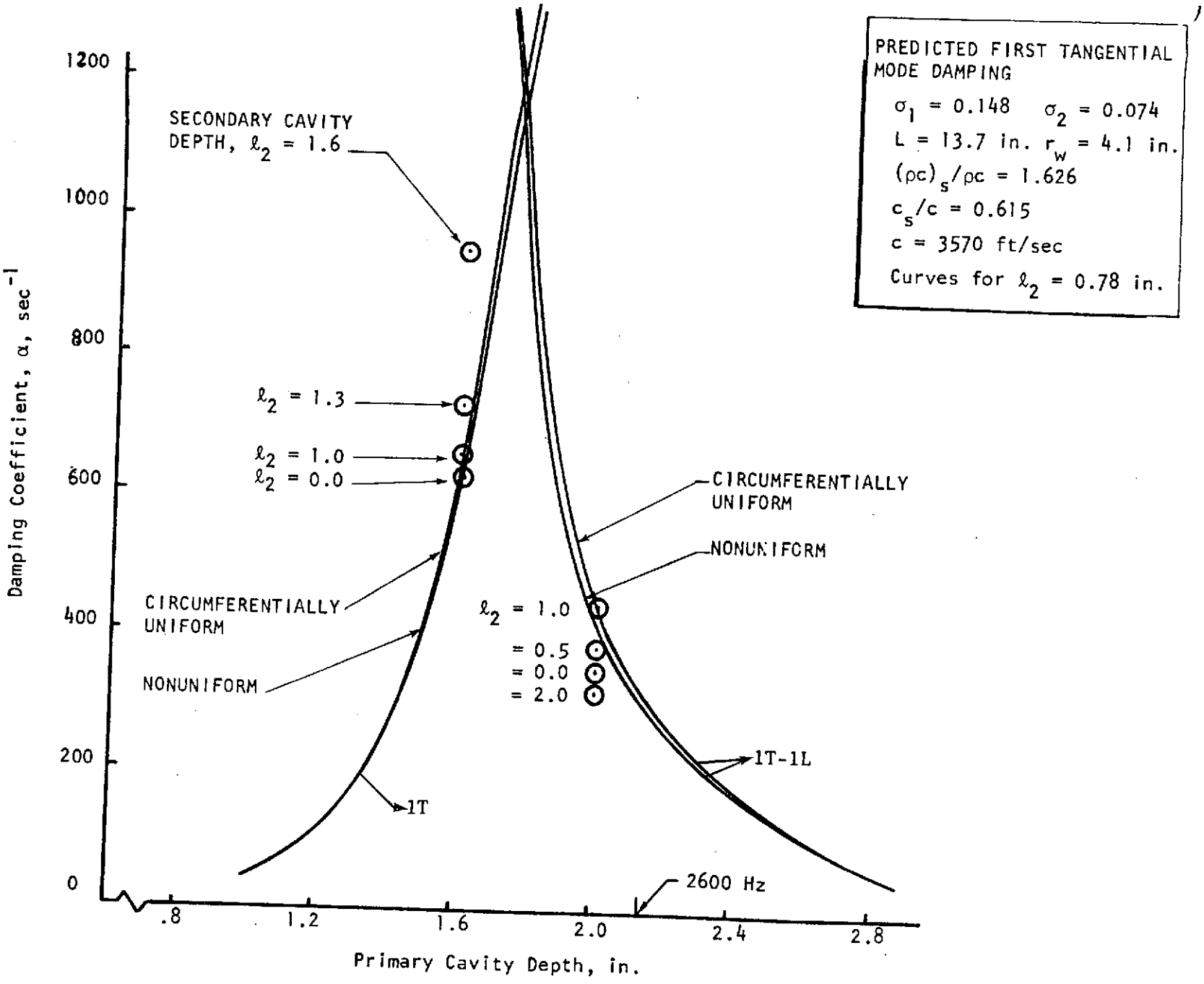


FIGURE 16. PREDICTED CAVITY DAMPING

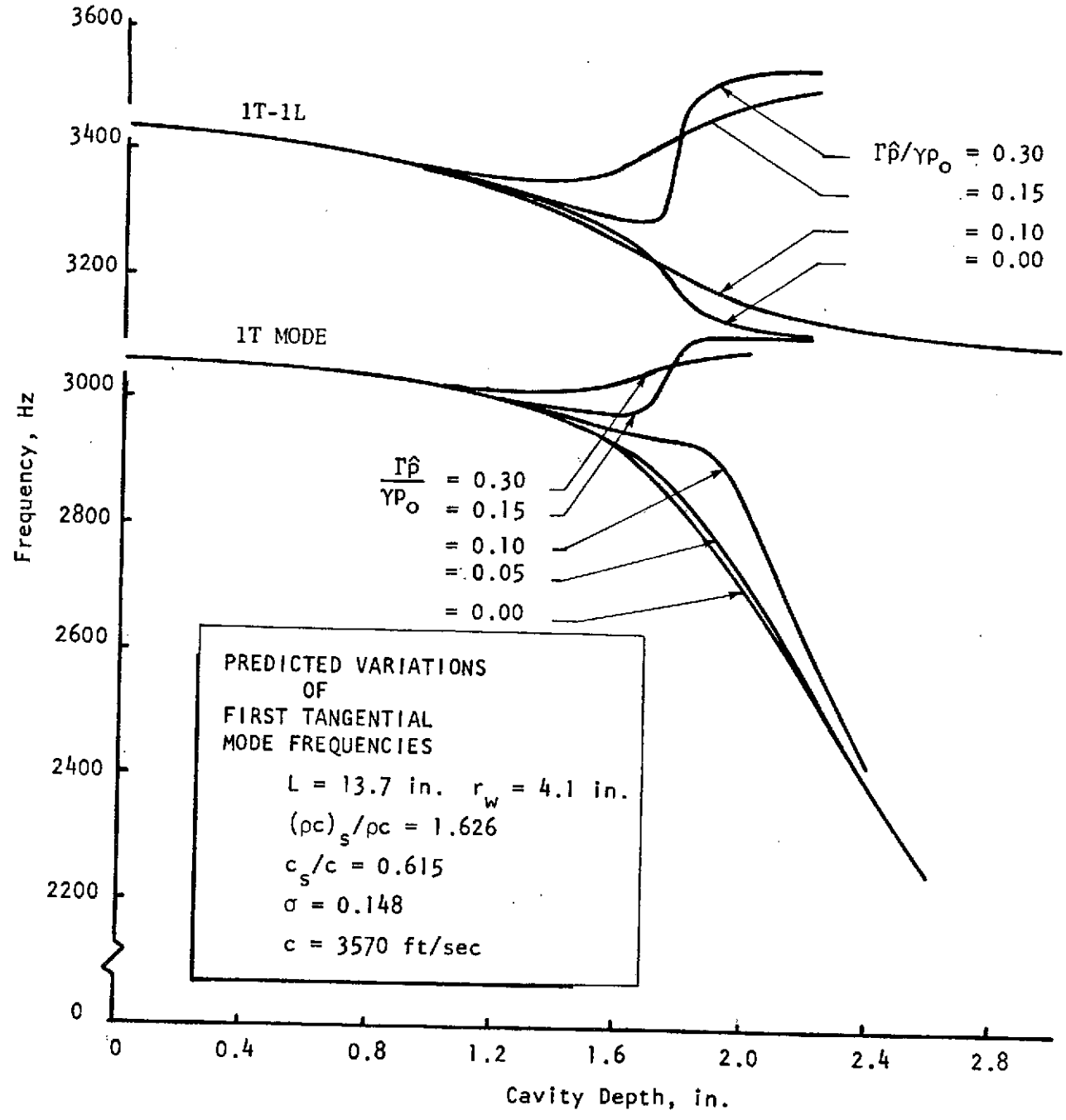


FIGURE 17. VARIATION OF PREDICTED FREQUENCIES WITH CAVITY DAMPING

If the low frequency mode is due to cavity effects alone, it is of interest to calculate the corresponding oscillatory pressure distribution within the combustion chamber. The calculated axial variationals of the pressure distribution for the 1T and 1T-1L modes are shown in Fig. 18. These results show that the oscillation is largely concentrated near the injector face for depressed frequency 1T mode, shown by curves for frequencies of 2808 and 2513 Hz. The remaining curves, corresponding to the 1T-1L mode, show the change in sign (phase) normally associated with a 1T-1L mode (shown for $\ell_1$ = 1.0 in.), does not occur with deep cavities ($\ell_1$ = 2.8 in.).

The foregoing analysis of cavity effects shows that frequencies of 2300 to 2900 Hz are possible as a result of cavity effects alone but very unlikely. Nevertheless, the results from full-scale testing, especially those obtained by Aerojet, show the cavity to have a significant effect under some circumstances. This observation suggests that cavity effects may interact with other effects, probably the feed system, to cause the 2300 to 2900 Hz oscillation. The nature of the calculated pressure distribution for the low frequency mode shown in Fig. 18 could be significant for interactive effects, because the pressure distribution is nearly equivalent to that calculated for a passive chamber driven from the injector end.

ANALYSIS OF FEED/INJECTION SYSTEM ACOUSTICS

An indication of the possibility of feed system oscillation in the frequency range of 2300 to 2900 Hz can be obtained from a calculation of the simple (uncoupled) resonant frequencies of various portions of the system. These frequencies (first tangential modes) for the Rocketdyne L/D #1 injector are shown in Table 5.

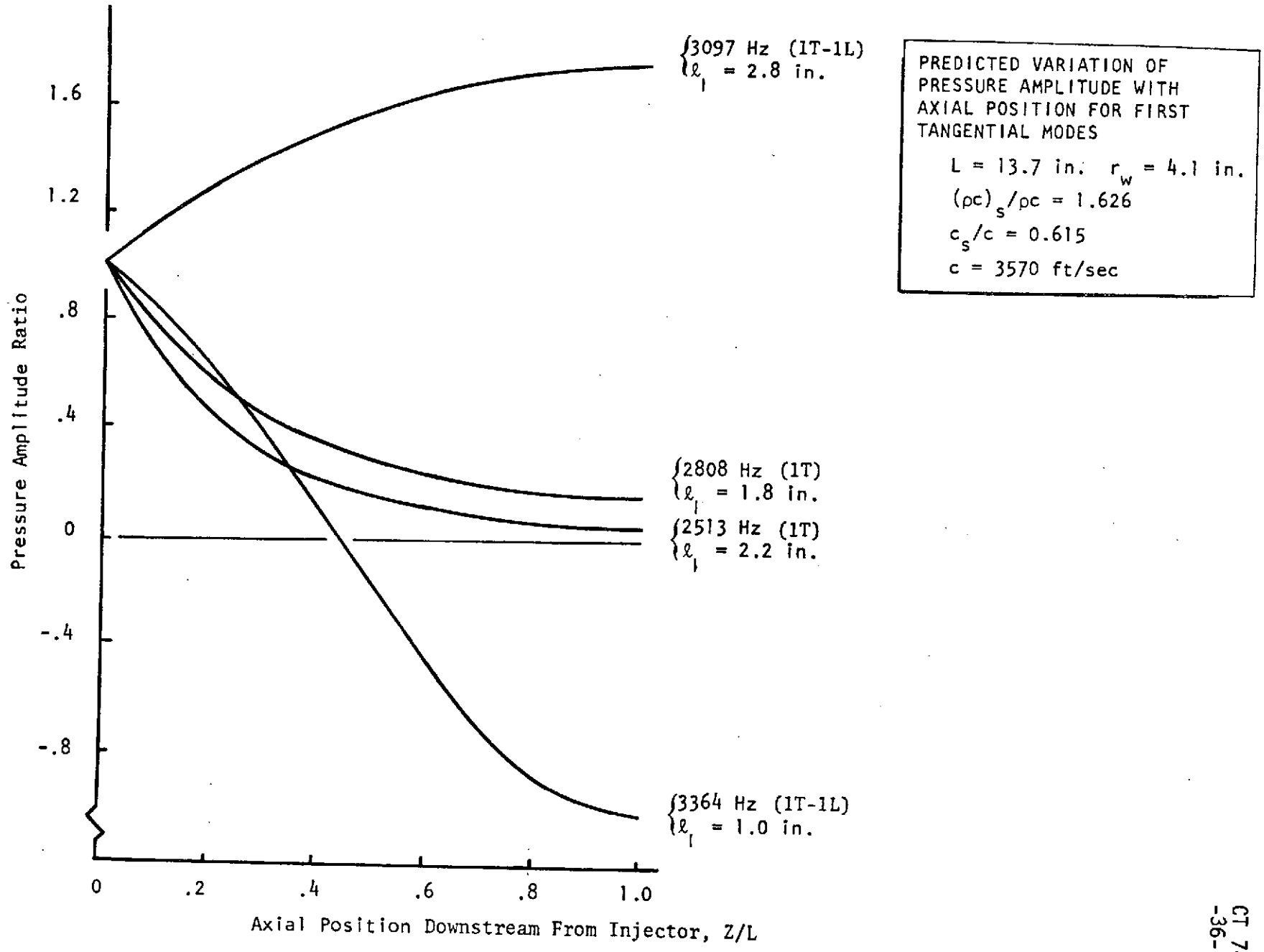


FIGURE 18. PREDICTED VARIATIONS OF AMPLITUDE WITH AXIAL POSITION

TABLE 5. CALCULATED UNCOUPLED RESONANT FREQUENCIES OF INJECTOR PASSAGES

| | Ring No. | $\bar{D}$, in. | $f_o = c/\pi\bar{D}$, Hz |
|---|---|---|---|
| Fuel System | | | |
| ↓ | 2 | 1.84 | 8502 |
| | 4 | 3.37 | 4768 |
| | 6 | 4.85 | 3313 |
| | 8 | 6.33 | 2538 |
| | 10 | 7.85 | 2047 |
| | Manifold | 6.7 | 2398 |
| Oxidizer System | | | |
| ↓ | 1 | 1.21 | 9911 |
| | 3 | 2.63 | 4560 |
| | 5 | 4.11 | 2918 |
| | 7 | 5.59 | 2145 |
| | 9 | 7.11 | 1687 |
| | Manifold | 2.35 | 5103 |

The frequencies shown in this table suggest that possibly fuel ring No. 8, the fuel manifold and oxidizer ring No. 5 could contribute to oscillations in the 2300 to 2900 Hz range.

These results suggested the need for a more thorough analysis of the feed system, allowing for coupling between the components. Therefore, such an analysis was developed. This model was obtained by solving the wave equation for the system sketched below:

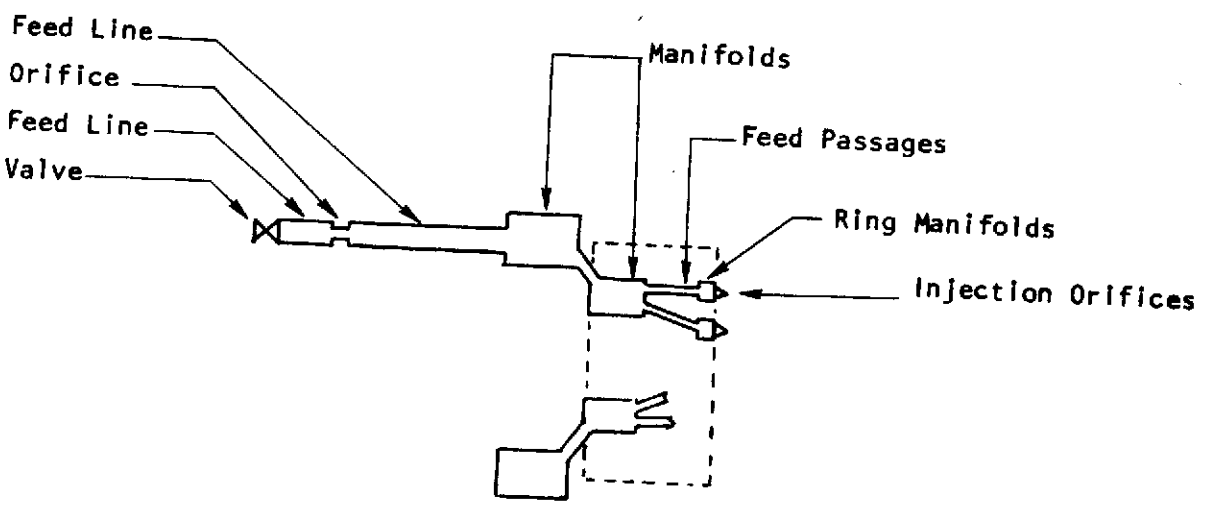

Allowance was made for transverse modes in the manifolds and one-dimensional wave motion in the feed lines and interconnecting passages. The injector passages and manifolds for L/D #1 are shown more fully in Fig. 19. A computer program was used which sequentially solved equations for each region of the form

$$\tilde{p}_i = A_i \cos k_m^{(i)} z_i + B_i \sin k_m^{(i)} z_i$$

$$\tilde{u}_i = -\frac{j}{\rho c} \frac{k_m^{(i)}}{k} \left[ A_i \sin k_m^{(i)} z_i - B_i \cos k_m^{(i)} z_i \right]$$

These equations were related at the interface between each region by

$$\tilde{p}_{i+1} = \tilde{p}_i + Z_i \tilde{u}_i$$

$$\tilde{u}_{i+1} S_{i+1} = \tilde{u}_i S_i$$

where $Z_i$ is an acoustic impedance. Relationships for this impedance of the form

$$Z = \overline{\rho} c (\theta + j\chi)$$

$$\theta = \frac{3}{2} \frac{\overline{u}_o}{c} \frac{(1-\sigma)(1-\sigma^2)}{C_c^2} \qquad \text{(Orifice Expression as Example)}$$

$$= \frac{3 g_c \Delta \overline{p}_{loss}}{\rho \overline{u} c}$$

$$\chi = k(\ell + \delta_u + \delta_D)$$

$$\delta \simeq 0.48 (S)^{1/2} (1 - 1.25 \sigma^{1/2})$$

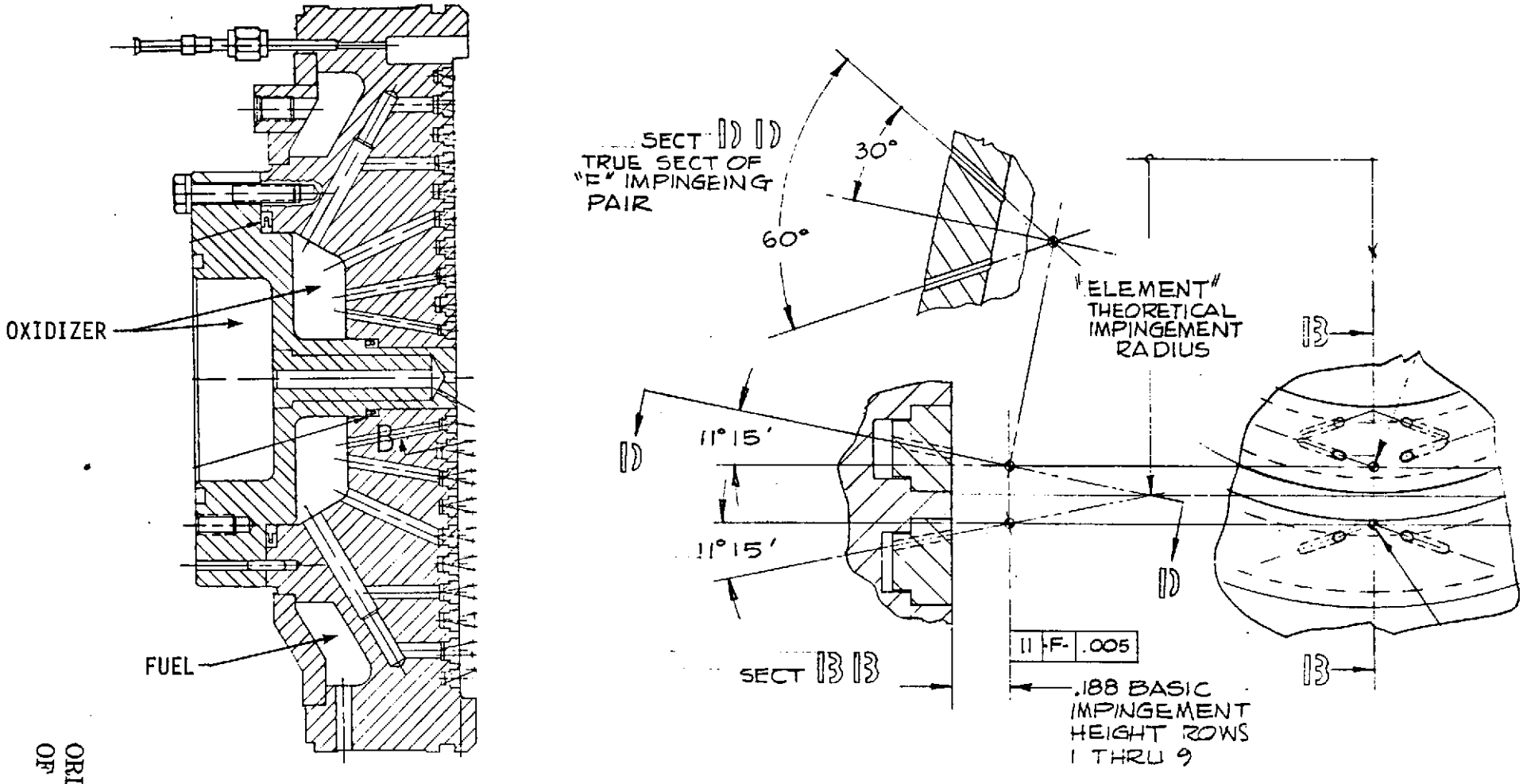


FIGURE 19. SCHEMATIC OF FLOW PASSAGES IN THE LIKE-DOUBLET NO. 1 INJECTOR

were used. This model was used to calculate resonant frequencies of the coupled injection systems, i.e., frequencies (complex) corresponding to zero pressure amplitude at the injector face were calculated. Although it has not been done, this calculation could be modified easily to calculate an injector admittance or transfer function of the type commonly used in the analysis of feed-system-coupled modes.

Calculations with this model for the fuel and oxidizer systems showed that a large number of modes were possible in the frequency range of interest. These modes varied with the assumptions used in the calculations. Calculated resonant frequencies for the fuel system are shown in Fig. 20 along with measured frequencies. The calculated curves are labeled for $m = 0$ or 1 which refers to the angular dependence of the mode as $\cos m\theta$, i.e., $m = 0$ corresponds to purely "longitudinal"-type modes and $m = 1$ corresponds to first tangential and "longitudinally" coupled (within the feed system) modes.

Although there are several modes with frequencies near those observed, the upward shift in frequency that occurred after installation of the manifold dams was not predicted. Indeed, a downward shift was predicted, as shown in Fig. 20. Therefore, the results from this analysis of the fuel system are not sufficient to firmly conclude the 2300 to 2900 Hz behavior is due to particular modes in this portion of the feed system. The results do show the large number of modes possible and suggest that further analysis could lead to an accurate prediction of observed behavior.

A similar analysis of the oxidizer system for purely longitudinal modes yielded the results shown in Fig. 21. These results appear more compatible with the observed behavior. However, re-examination of the test data from this program showed clear evidence of a first-tangential type of angular dependence of the pressure distribution. Thus, the results from the analysis of the oxidizer system do not permit the firm conclusion that the 2300 to 2900 Hz behavior is due to this portion of the feed system either.

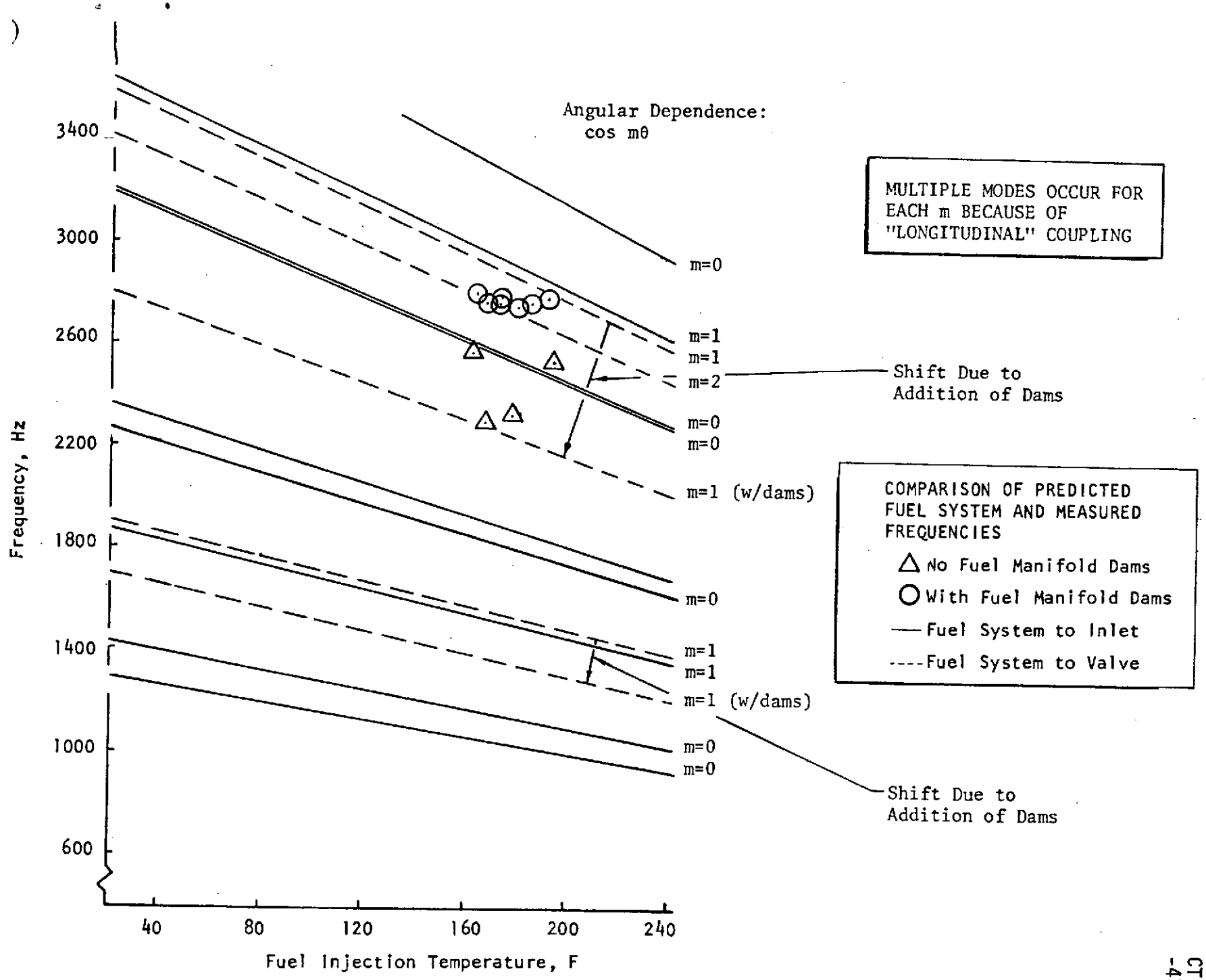


FIGURE 20. COMPARISON OF MEASURED FREQUENCIES WITH CALCULATED FREQUENCIES FOR FUEL SYSTEM

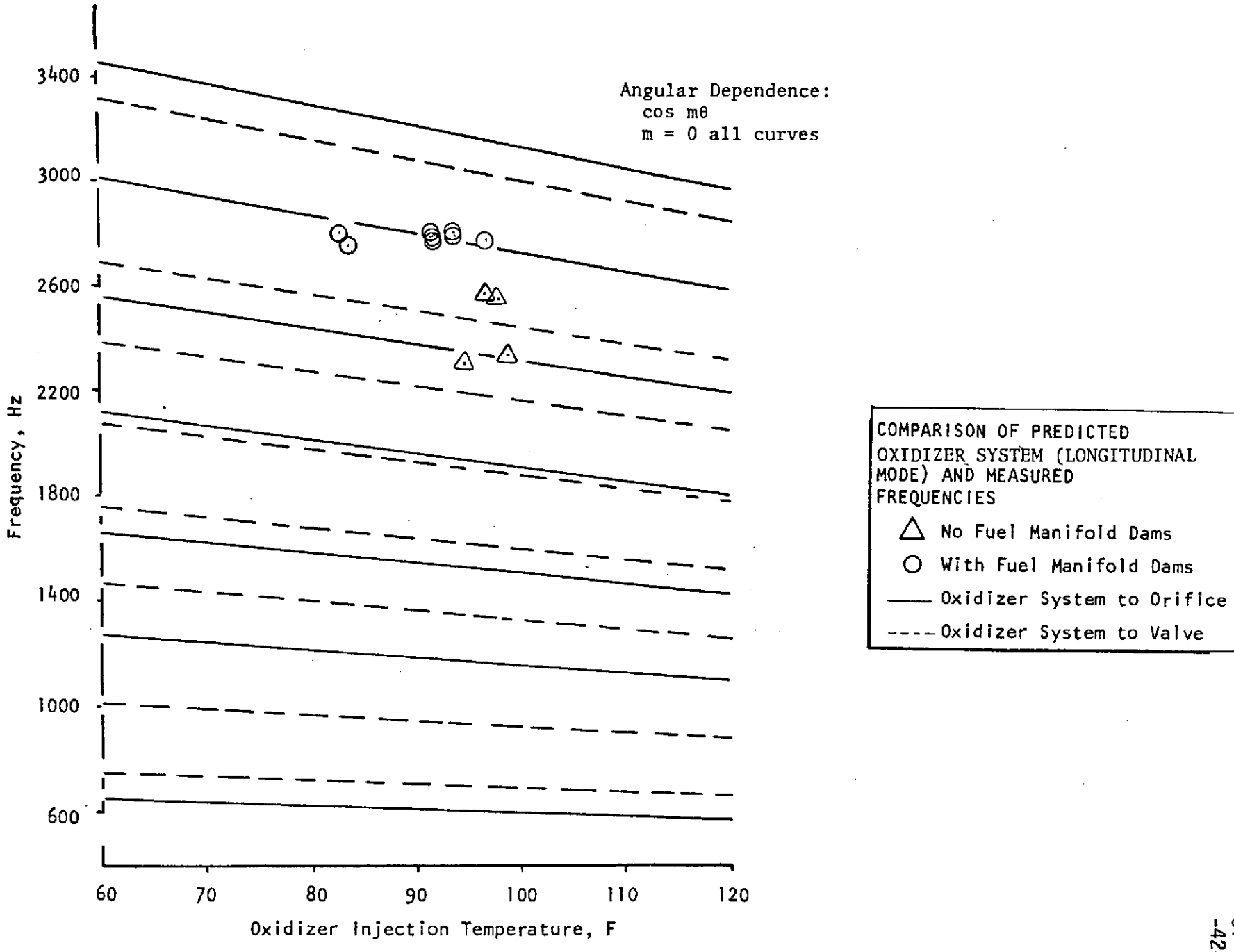


FIGURE 21. COMPARISON OF MEASURED FREQUENCIES WITH CALCULATED FREQUENCIES FOR OXIDIZER SYSTEM

OBSERVATIONS FROM 2300 TO 2900 HZ DATA

The 2300 to 2900 Hz instability data from the full scale firings may be grouped into three sets:

1. A 2300 Hz oscillation appeared briefly during the decay transient after two bombs. The phase angles suggest a first-tangential angular distribution of pressure.

2. Two sustained instabilities occurred with frequencies near 2560 Hz. The amplitude and phase data suggest a precessing and then standing first tangential-type pressure distribution. The pressure node appeared to stand along the fuel inlet line. The amplitudes were ~35 to 70 psi peak to peak.

3. After installation of the manifold dams, multiple occurrences of a 2790 Hz oscillation were encountered. In each case the oscillation damped in 10 to 70 milliseconds. The amplitude and phase behavior suggested, as with the 2560 Hz oscillation, that the mode precessed initially and then stood with the pressure node along the fuel inlet. Amplitudes were ~50 to 150 psi peak to peak.

Conclusions Regarding 2300 to 2900 Hz Oscillation

Results from the analysis effort do not permit the mode or modes of oscillation to be identified fully. However, it appears very unlikely that this oscillation is caused by cavity effects alone. Nevertheless, the oscillation is influenced by the cavity entrance configuration. This oscillation is also influenced by dams in the fuel manifold and, in addition, it appears to have a first-tangential-type of pressure distribution with the nodal position influenced by the fuel inlet position. These results suggest that the oscillation is associated with an interaction between the fuel injection system and cavity effects. The cavity influence may result from interaction between the oscillatory jet emerging from the cavity and the injection/combustion processes of adjacent injection elements.

The available test data suggest that this mode has not occurred in the 10-inch-diameter chambers.

Summary of Other Analytical Results

Based on the comparison of measured and predicted frequencies in the chamber acoustic model, the ability to properly predict the effects of cavities of chamber mode frequencies has been confirmed.

In addition, modifications were made to an existing computerized model to predict the damping from circumferentially nonuniform cavities.

Also, the results from the acoustic analysis of the fluid systems encourages further work.